

Final Project
2.2-2.4 GHz Phased-Array Conceptual
Redesign

by **Russell Hofer**

May 2005

Table of Contents

ACKNOWLEDGEMENTS	1
INTRODUCTION.....	2
BACKGROUND OF EXISTING ANTENNA ARRAY	2
REDESIGN OBJECTIVES	6
INCREASE ANTENNA BANDWIDTH.....	7
<i>Increase of Antenna Element's Bandwidth.....</i>	<i>7</i>
<i>Increase of Bandpass Filters' Bandwidth</i>	<i>13</i>
CONCEPTUAL REDESIGN OF ANTENNA ELEMENT PCB	18
<i>Steering Redesign.....</i>	<i>18</i>
<i>Schematic Redesign.....</i>	<i>24</i>
TRANSMIT CAPABILITIES	29
TRANSMIT CAPABILITIES	30
CONCLUSIONS	39
FURTHER WORK.....	40
REFERENCES.....	41
APPENDICES	42
<i>Appendix I: Matlab Code</i>	<i>42</i>
<i> Figure 9.....</i>	<i>42</i>
<i> Figure 17, 18.....</i>	<i>42</i>

Acknowledgements

I would like to acknowledge Dr. Christopher Allen for his guidance through this project. In addition, I would like to thank Mr. Dan Depardo for his willingness to answer questions and share his valuable experience of antenna and microwave design. Lastly, Dr. Jim Stiles for consultation on general microwave principles and providing what has proven to be a very useful course in microwave design.

I would like to extend a thanks to Dr. Christopher Allen, Dr. Prasad Gogineni, and Dr. Kenneth Demarest for participation in my committee.

Last, but not least, I would like to extend my gratefulness to my wife, Kristie Hofer, for her support and patience.

Introduction

In 2004, Kansas University and Honeywell FM&T Kansas City Plant jointly built a 2.3-2.4 GHz Phased-Array Prototype. Mr. Dan Depardo, RF electronics engineer, was responsible for the design, construction, and preliminary testing. The antenna has proven to perform adequately per its original design criteria. However, Dwayne Brown, KCP (Kansas City Plant) product engineer, has extended requirements that are to be incorporated into the second design iteration. In this report, the results of the conceptual redesign of the antenna array are discussed. Included is a brief background of the existing antenna array, redesign objectives, new antenna design, simulation results, and further work/conclusions.

Background of Existing Antenna Array

The following discussion gives a limited overview of the original antenna array design. The interested reader is referred to [1] for a detailed overview. The original antenna consists of eight patch elements positioned in a linear array. The array is capable of performing electronic steering in azimuth. The bandwidth of the antenna encompasses 2.3-2.4 GHz. Figure 1 shows an image of the original 2.3-2.4 GHz phased-array antenna prototype [1].

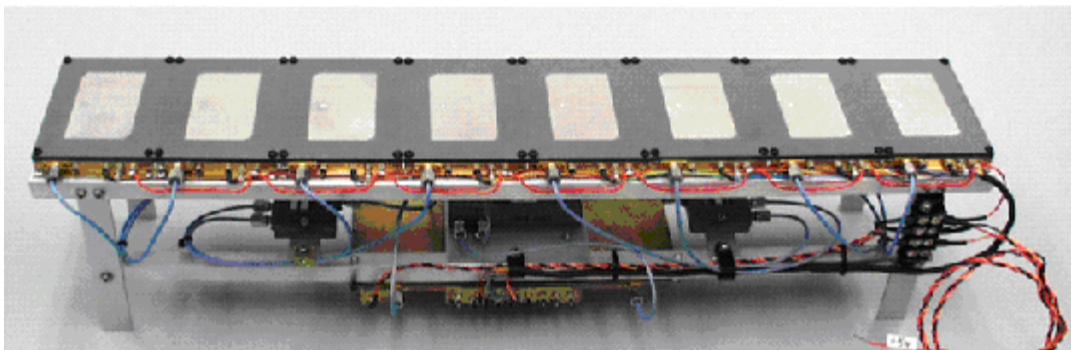


Figure 1: 2.3-2.4 GHz Phased-Array Antenna Prototype

Each patch antenna element consists of a low-noise RF amplifier, two-stage RF bandpass filter (100 MHz B/W), two variable voltage phase shifters, and further small-signal RF amplification. Figure 2 shows a basic block diagram of the antenna element. Notice that each antenna element must be given a steering signal. This signal controls the amount of phase shift incurred by the RF signal at each element.

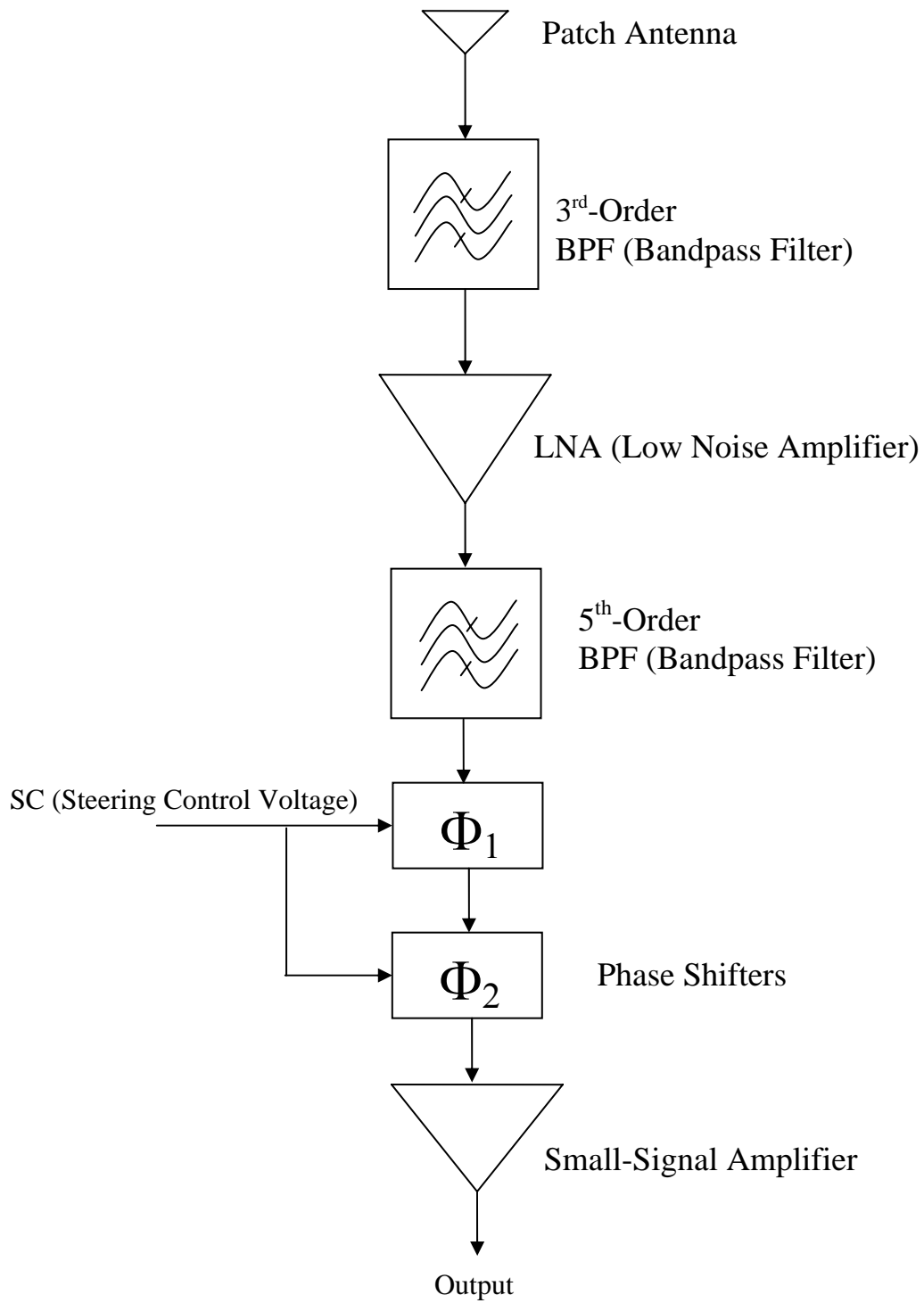


Figure 2: Block Diagram of an Antenna Element

Ideally, each antenna element will have a constant delta phase shift with respect to its neighboring elements given by Equation 1 [2]:

$$\Delta\theta = 2\pi d / \lambda * \cos\theta_0 \quad (1)$$

d = interelement spacing

λ = wavelength

θ_0 = steering angle

For a broadside beam, there is no relative phase shift per element. The steering control voltage, depicted in Figure 2, is generated by an analog op-amp array. This circuit generates a maximum delta steering voltage between elements of approximately 1 volt. Assuming the phase shifters' behavior is roughly linear, this results in a maximum delta phase shift between elements of approximately 30 degrees. Also, the distance between elements with respect to wavelength is approximately 0.23. Using this information in Equation 1, the maximum obtainable steering angle is +/- 20 degrees from broadside.

The signals from all antenna elements are combined with two RF power combiners and a 180° hybrid coupler. These signals, one given the designation 'SUM RF' and the other 'DELTA RF' are routed onto the RF Signal Processor board. Additional functions of the RF signal processing board are to provide additional variable gain, sum level, and delta level detection as follows. Both the 'DELTA RF' and the 'SUM RF' signal are further amplified with a variable gain amplifier. Both signals are then sampled using a bi-directional coupler. The sampled signal is used for level detection. The detected signals are given the name 'SUM LEVEL' and 'DELTA LEVEL'. The purpose of the 'SUM LEVEL' and 'DELTA LEVEL' signals are to determine the strength of the received signal and the direction of the transmitter. The 'DELTA LEVEL' signal has the desirable attribute that it provides a sharp null when the antenna is steered in the direction of the transmitter. This allows for accurate tracking. The RF signal processing board interacts with a user supplied digital control system as depicted in Figure 3.

Figure 3 shows an overview of the original system. As can be seen from Figure 3, the user supplied digital control system provides the RF signal processor with a steering control voltage. The RF signal processor subsequently provides each element with a steering control voltage. The control voltage is directly applied to each element's set of phase shifters. The digital control system is also responsible for interpreting the 'SUM LEVEL' and 'DELTA LEVEL' signals. Based upon its interpretation, it may vary the gain of the RF Signal Processor's variable gain amplifier and/or adjust the steering control.

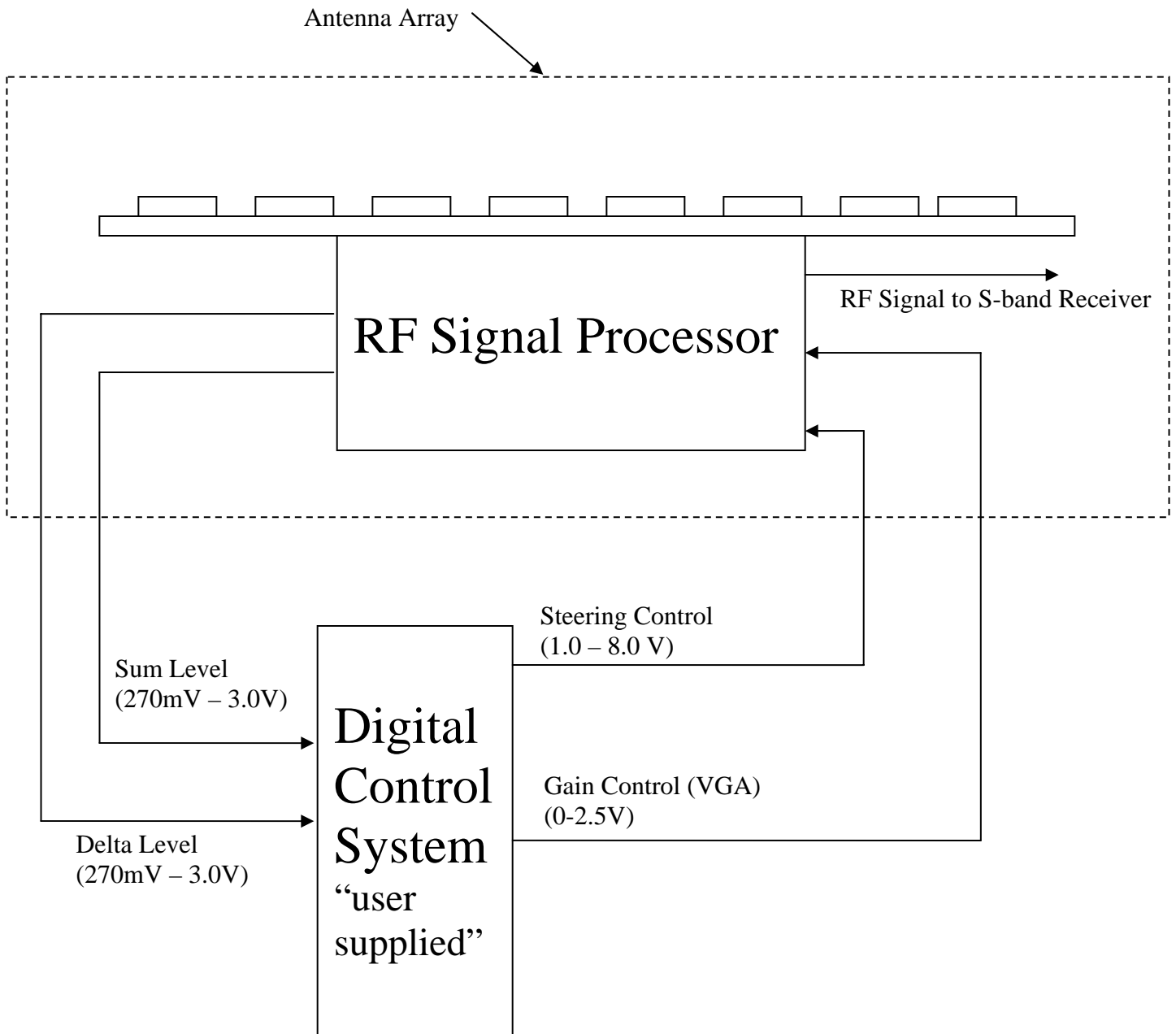


Figure 3: Top Level Block Diagram

Redesign Objectives

The following list details the redesign objectives:

- Maximize antenna gain / efficiency
- Increase antenna bandwidth to 200 MHz covering 2200-2400 MHz
- Maximize steering angle
- Variable beamwidth (controllable)
- Increase dynamic range of antenna
- Add dual mode capabilities – transmit & receive at 10 W
- Transmission and reception must operate in duplex mode

The following list details personal objectives to be gained at the end of this project:

- Expertise in antenna design
- Learn antenna design CAD software (HFSS)
- Learn RF microwave design software (ADS)
- Perform simulations in both antenna design software and RF microwave design software
- Increase familiarity with RF microwave design terminology

Initially, the following schedule was adopted to perform the described objectives:

Research and determine best CAD software to use, obtain license if needed	Oct 2004
Attend course to learn CAD software, pending availability of course	Dec 2004
Attend course to learn RF microwave design software	Dec 2004
Literature search and review of the topic	Feb 2005
Modify element design to include increased bandwidth	April 2005
Modify array design & create transceiver design (Deliverable is a proof of concept / virtual prototype; conceptual schematic & geometry)	May 2005
Produce a hardware prototype (if possible)	May 2005

Increase Antenna Bandwidth

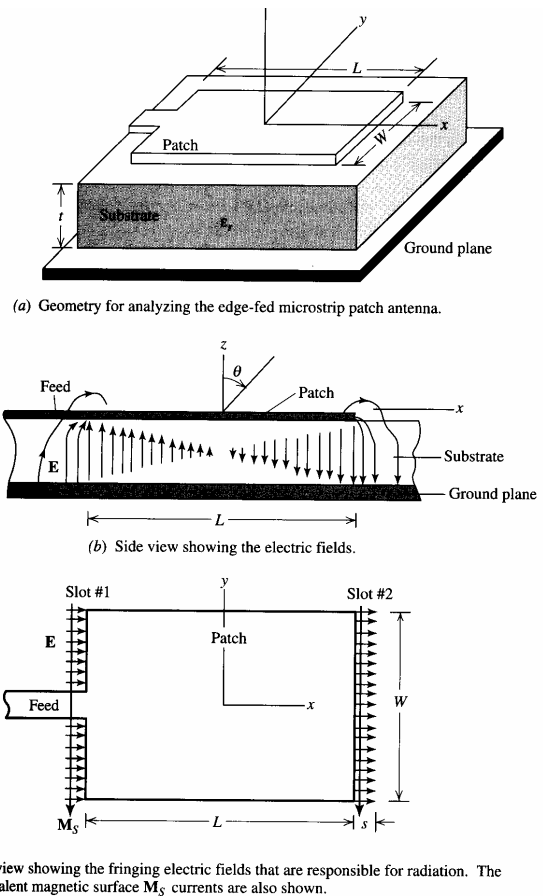
In order to increase the antenna bandwidth, two things must be realized. The antenna patch element bandwidth must operate at 2200-2400 MHz; all electronic components must satisfy the increased bandwidth requirement. This means that the bandwidth of both the first and second stage bandpass filters must be increased.

Increase of Antenna Element's Bandwidth

Each antenna element consists of a single layer patch antenna. A number of different approaches are available to increase the bandwidth of patch antennas. The most common involve the use of cavities and stacked substrate techniques [3]. However, these techniques increase the complexity, size, and weight of the design. The simplest approach is to increase the height of the substrate. The drawback to this approach is that if the height is made too tall, an increase in the production of surface waves will decrease the antenna's efficiency.

The strategy to be employed is to moderately increase the height of the patch antenna in order to achieve the desired increase in bandwidth. Figure 4 shows the geometry of a typical patch antenna. Figure 4 is close to the original configuration, with the exception that the patch antenna was fed using a coaxial probe. More discussion with regards to Figure 4 will be given in the proceeding paragraphs.

The basic design equations used are given by [5]. A brief overview of the design strategy is included in this report. For more detailed information, the interested reader is referred to [5]. The model used throughout the design process consists of the 1st order transmission-line model. Some of the concepts of the cavity model are also deployed. The transmission-line model assumes that the patch antenna may be treated as a transmission line with an open circuit at each end of the transmission line. These 'open circuits' are the radiating apertures of the patch antenna. Since the end apertures radiate and subsequently are lossy, this is only a rough approximation. The length of the patch antenna is chosen so that the transmission line transforms the total admittance of the open circuit ends to a real impedance. It can be shown from transmission line theory that this is approximately $\lambda/2$. It is actually somewhat less to account for fringing/radiating effects.



(c) Top view showing the fringing electric fields that are responsible for radiation. The equivalent magnetic surface M_s currents are also shown.

Figure 5-54 The half-wavelength rectangular patch microstrip antenna; $L \approx 0.49\lambda_d$.

Figure 4: Patch Geometry [4]

With the correct patch length, a real impedance is obtained. Now, the real input impedance can be matched to the line impedance feeding the patch. In the case of a coaxial feed, this is best illustrated by observing Figure 4. When the patch is in resonance, the electric field will be as depicted. As can be seen, the E-field is a maximum at the two edges of the patch antenna. The current will be close to zero at the two edges of the patch and a maximum at the center. Consequently, the impedance will be close to 0 at the center and relatively large at the ends. It can be shown that an approximate relation is given by the following equation [5]:

$$Rin(y = y_0) = Rin(y = 0) * \cos^2\left(\frac{\pi}{L} y_0\right) \quad (2)$$

Thus, if one moves the coaxial feed lengthwise with respect to the patch, a resonance point may be found. The design strategy employed is as follows. Initially, the patch height is increased. The coaxial feed is centered along the width of the patch antenna. The coaxial feed is moved lengthwise along the patch until resonance is achieved at any arbitrary frequency. The patch length is adjusted to achieve resonance at the desired frequency of 2.3 GHz. An iterative procedure is necessary, as second order effects relate all design parameters; for example, adjusting the length of the patch antenna will slightly alter the required feed location.

In the original design, the patch height was set to 0.15". The height was chosen due to the availability of excess material from another research project. The original dielectric material was Rogers Dielectric 5870, with a relative dielectric constant of 2.33. Rogers Corporation only carries standard sizes up to 0.125" thick. After contacting the manufacturer, they were able to verify availability of Dielectric 5880, 0.25" thick. This material has a slightly lower loss factor compared to 5880, with a relative dielectric constant of 2.2. It was decided that this would be a good candidate for the design.

HFSS was used to model the antenna's performance. The original model was developed using an example from [6]. The design model is depicted in Figure 5. The initial model used idealizations in order to improve simulation speed. These assumptions were later relaxed during final simulations. Assumptions include all conductors being

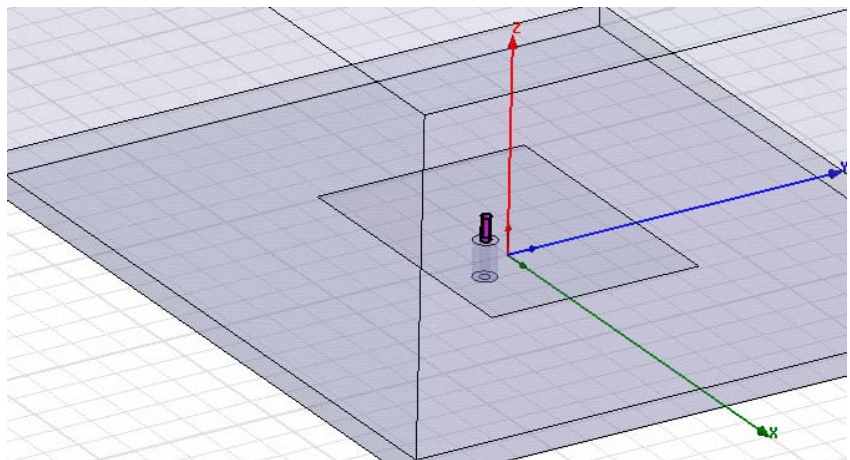


Figure 5: Patch Geometry

PEC (perfect electric conductors), the ground plane being infinite in extent, and a reduced size radiation boundary. The simulated antenna was totally enclosed in an air box, as depicted in Figure 5. The walls of the box are assigned as the radiation boundary. A larger radiation boundary will yield more accurate results. According to HFSS documentation, the following requirements should be met for the radiation boundary to accurately simulate open space: 1) the radiation boundary must be greater than $\frac{1}{4}$ wavelength from any radiating surface; 2) boundary orientation must be set perpendicular to incident radiation. These requirements were met to a fair degree; during final prove-in of the simulation, they were improved.

The patch height was increased to 0.25" using Dielectric 5880 as the substrate. The coaxial feed was centered along the width of the patch antenna. A failed attempt was made to move the coaxial feed lengthwise along the patch to reach resonance. After a great deal of consideration, it was determined that the increased probe length was introducing too much inductance into the feed. See Figure 6.

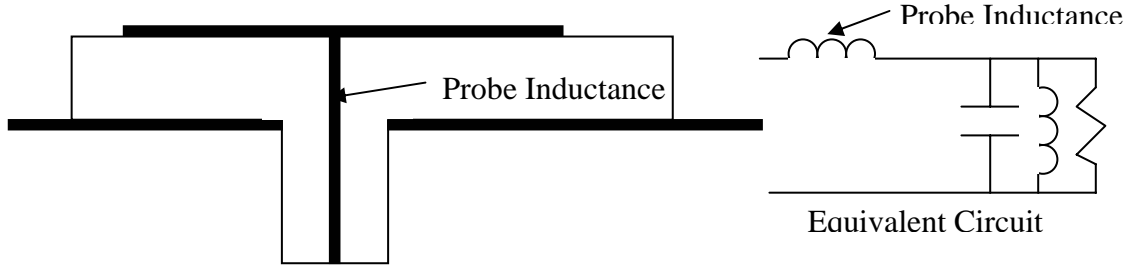


Figure 6: Probe Inductance

Two simple methods are available to counteract the introduced inductance. The first method is that a gap may be introduced between the probe and the patch. This will add a capacitance that negates the inductive reactance at the design frequency. Second, the probe width may be increased. This minimizes the inductance of the probe. The first method was too sensitive to design deviations. The second technique was found to be adequate. It was verified that a probe radius of 0.15 cm could achieve a reasonably good 50-ohm match. A probe radius of 0.15 cm corresponds to a 3 mm wide probe. This may be difficult to solder onto the patch due to heat dissipation, but construction should still be feasible. In addition to increasing the height, it can be shown that increasing the patch width lends towards an increase in bandwidth. Unfortunately, it was experimentally determined that an increase in patch width also increases inductance. Consequently, the patch width was also reduced from 6.239 cm to 6 cm in order to minimize inductance to achieve an acceptable impedance match.

The final patch dimensions can be summarized as follows. The dielectric height is 0.25"; the patch width is 6 cm; the probe radius is 0.15 cm; the patch length is 3.913 cm. The patch is fed using an inset of 0.75 cm from the edge (this is the distance from the patch's edge to the radial center of the coaxial feed). The final simulation was made more realistic by using the patch's true conductor (finite thickness copper). The simulation volume was also expanded to include ~ 2 wavelength width radiation boundary (compared

to $\frac{1}{4}$ wavelength in original simulation). The ground plane was reduced from being infinite in extent. The resulting simulation took ~ 30 minutes per iteration. The simulated results were not drastically different from the ideal simulations. We now proceed to describe the simulation results.

Figure 7 shows the impedance match as a function of frequency vs. VSWR.

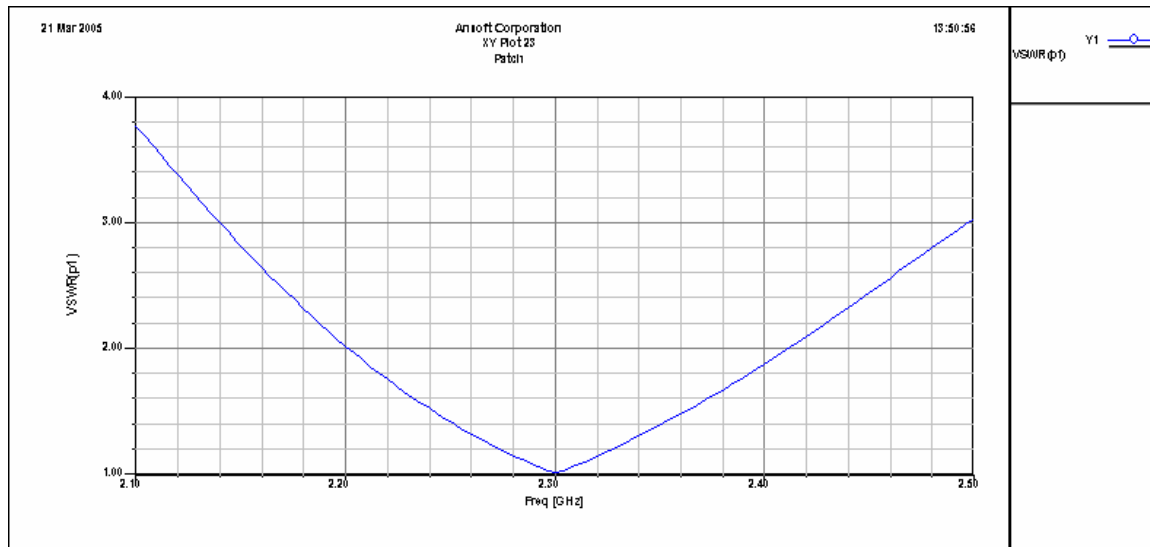


Figure 7: Antenna VSWR

As can be seen from Figure 7, the resonant frequency is centered at 2.3 GHz. The 2:1 VSWR band extends from 2.2-2.4 GHz. This will allow $\sim 90\%$ of the incident power to be transmitted into a 50-ohm matched transmission line.

Figure 8 shows a 3D plot of the radiation pattern in dB. As to be expected, the beam pattern is fairly symmetrical with respect to the z-axis. There is ~ 5 dB attenuation at ~ 60 degrees compared to the field calculated at broadside. This field is calculated with 1 W of incident power on the antenna's input port.

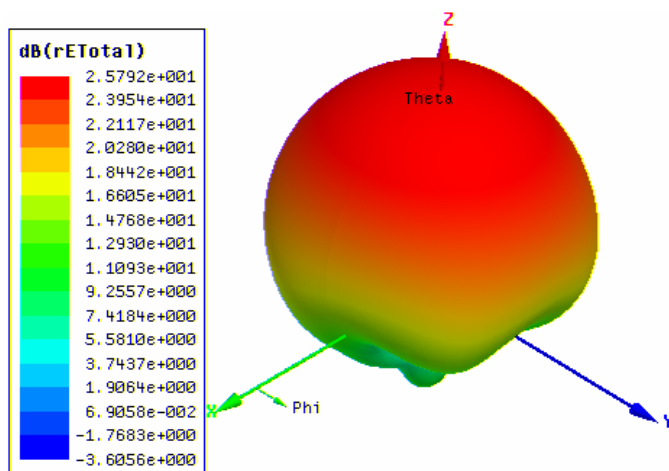


Figure 8: 3-D Polar Plot from Patch Antenna Element

In order to obtain a better estimate of the antenna's expected performance in a receiver, the realized gain is plotted vs. theta for phi=0,90 degrees. These results are shown in Figure 9. The realized gain is defined as follows:

$$realized_gain = 4\pi * \frac{U}{P_{incident}} \quad (3)$$

U = the radiation intensity in the specified direction (watts per steradian)

P_{incident} = the total incident power on antenna's input port (watts)

This definition of gain indicates the actual power/steradian radiated compared to that of an ideal lossless isotropic radiator. The realized gain pattern shown in Figure 9 does not include coupling effects between elements. Figure 7 & 8 were also created with no regards to coupling effects. Results shown in Figures 7, 8, and 9 will differ from actual results due to the presence of other neighboring antenna elements. Coupling effects are dependent upon frequency as well as the scan angle of the patch antenna [9]. It is possible that coupling effects could reduce the realizable steering angle of the patch antenna array. We will briefly consider the effects of coupling as follows. The patch elements are positioned collinearly in the E-plane. The distance between patch edges is ~3.6 cm. This yields a normalized edge separation with respect to wavelength of ~0.27. According to [5, p 765], this will yield an $|S_{12}|^2$ of ~-20 dB. This result shows that coupling effects are not expected to be a dominate factor. All subsequent results assume that coupling effects may be ignored. However, it is recommended that a simulation be performed to verify that coupling effects do not significantly alter the obtained results. A simulation should be performed to test the complete antenna array performance while the array is steered both at broadside and at a maximum steering angle.

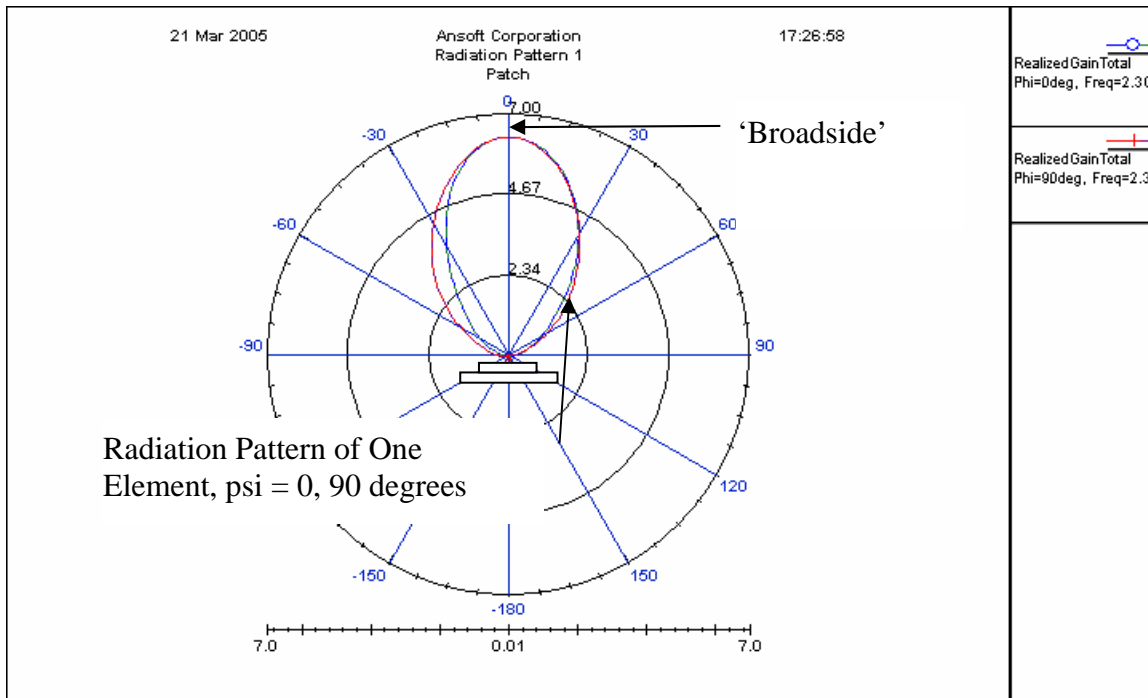


Figure 9: Realized Antenna Gain

In order to more easily model the gain of the system in subsequent discussion, we will proceed to calculate an approximate relationship for the antenna gain with respect to θ . A good first order approximation for gain will have the following form [4, p 213]:

$$realized_gain = max * \cos(\alpha * \sin(\theta)) \quad (4)$$

α =constant

max=maximum realized gain

Curve fitting to Equation 4 was accomplished by setting the maximum value to 6.32 dB as read from Figure 9. In order to obtain α , an arbitrary reading from $\theta=60$ degrees was used. Figure 10 was obtained by plotting the described expression in Matlab (see Appendix I for the actual code).

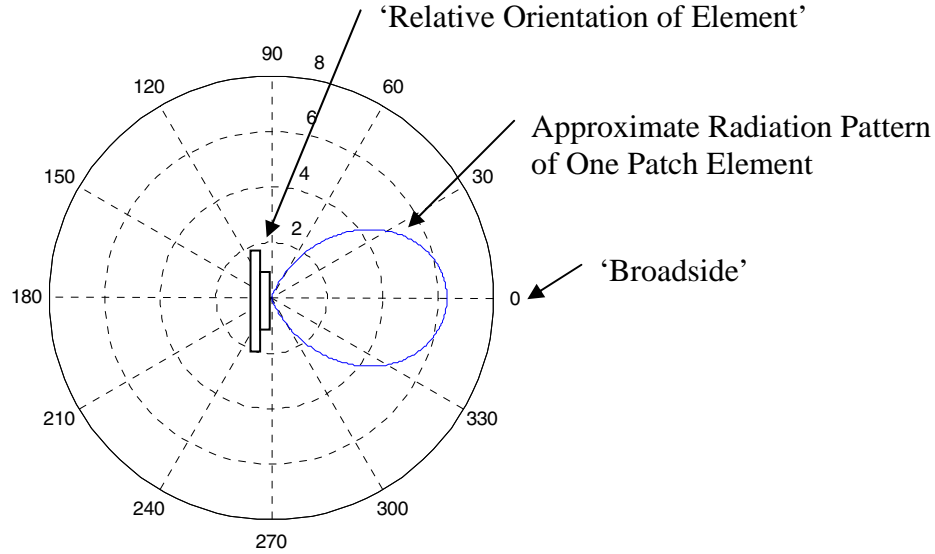


Figure 10: Approximate Antenna Gain

Comparison of Figure 9 and Figure 10 reveal that this approximation is reasonable. This approximation will be used in subsequent discussion of the overall system performance to include the effects of the array.

Increase of Bandpass Filters' Bandwidth

In order to increase the antenna bandwidth, all electronic components must satisfy the increased bandwidth requirement. This means that both the first and second stage bandpass filters must be modified.

The original PCB layout contains two bandpass filters. The first bandpass filter is of 3rd-order, placed directly after the antenna input, while the other bandpass filter is of 5th-order directly after the low noise amplifier. It might be noted that placement of a filter before the low noise amplifier does not follow conventional design. The purpose

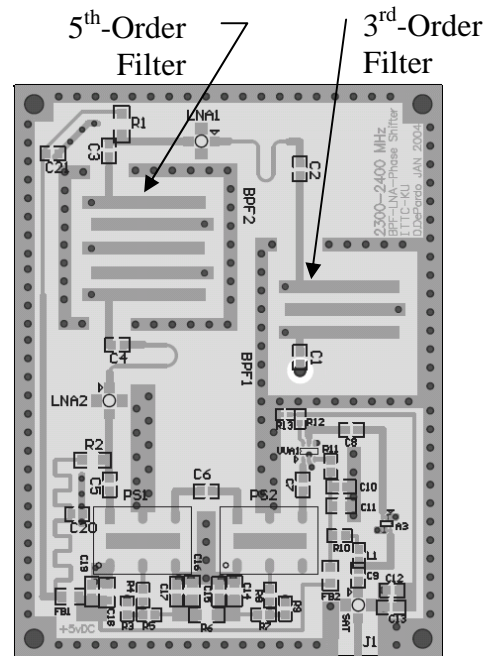


Figure 11: PCB Layout

of the 3rd-order filter is to attenuate signals in the 2400-2500 MHz band (802.11 WLAN traffic) to an acceptable level.

This type of filter is referred to as an Interdigital Connect Filter. The interested reader is referred to [7] for a more detailed discussion of this filter type.

The first design strategy was to use the built-in wizard contained within ADS design software. The process involves specifying both the upper and lower pass and stop bands. The maximum allowable passband attenuation and the minimum allowable stopband attenuation are also specified. The filter order may be specified; if it is not, the wizard will calculate the minimum order needed to meet the requirements. Lastly, the response type may be specified as maximally flat, or Chebychev. An example of the best obtainable output for a 5th-order filter is presented in Figure 12. This result was obtained after considerable tuning of the input parameters. As can be seen, the resulting filter is not acceptable. There is a 5 dB notch in the center of the passband. The reason for this unacceptable behavior is unknown. It appears that Agilent may not have thoroughly tested this design guide for robustness. Similar results were obtained with the 3rd-order filter.

The original filter design was made using a product from Eagleware. Unfortunately, this software was unavailable for immediate use. An alternative solution was to make use of optimization features contained within ADS. This solution proved to be a bit tedious to setup, but once setup it is extremely flexible and effective.

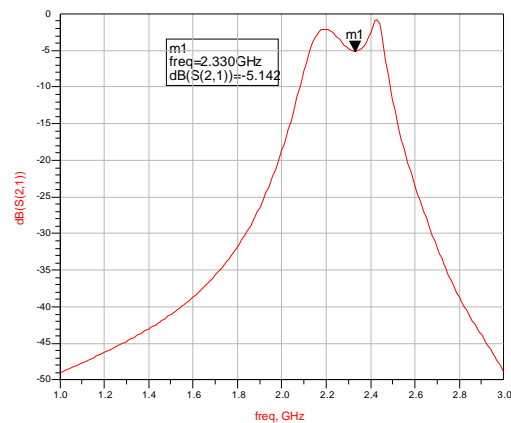


Figure 12: 5th Order Filter Response using Built-in ADS

Figure 13 shows the optimization circuit for a 5th-order filter. As can be seen, there are a total of four goal objects. The goal objects make reference to 'stop1', 'stop2', 'avg', and 'delta'. 'Stop1' refers to the stopband attenuation found at the lower stopband frequency. 'Stop2' refers to the stopband attenuation found at the upper stopband frequency. 'Avg' refers to the average attenuation within the passband. 'Delta' refers to the maximum-minimum passband attenuation. Specific definitions of these variables are defined underneath the Meas Eqn object in the lower right hand corner. The optimization object, 'Optim', makes references to all of the defined goal objects, determines the search algorithm, weighting, and other options. All goals are each assigned an acceptable level. For instance, if the lower stopband is less than 40 dB, no penalty is incurred. If all goals are found to be within their acceptable level, 'perfect' optimization is achieved and optimization stops. In most situations, the designer is trying to obtain the 'best' possible solution with conflicting goals; consequently, acceptable levels may be set in such a way that the optimization does not reach an optimal value. In this scenario (this also describes the current filter optimization), the ability to weight goals relative to their importance level is a critical feature. This was taken advantage of in order to obtain a steep rolloff in the upper stopband edge of the 3rd-order filter (to remove as much 802.11 interference as possible). When the optimization cannot reach a 'perfect' optimization, the optimizer may be set to a maximum number of iterations. Lastly, another interesting feature of ADS's optimization is the ability to see the results within a data display in real-time as the optimizer performs iterations. This facilitated troubleshooting/tuning of parameters to obtain the desired results.

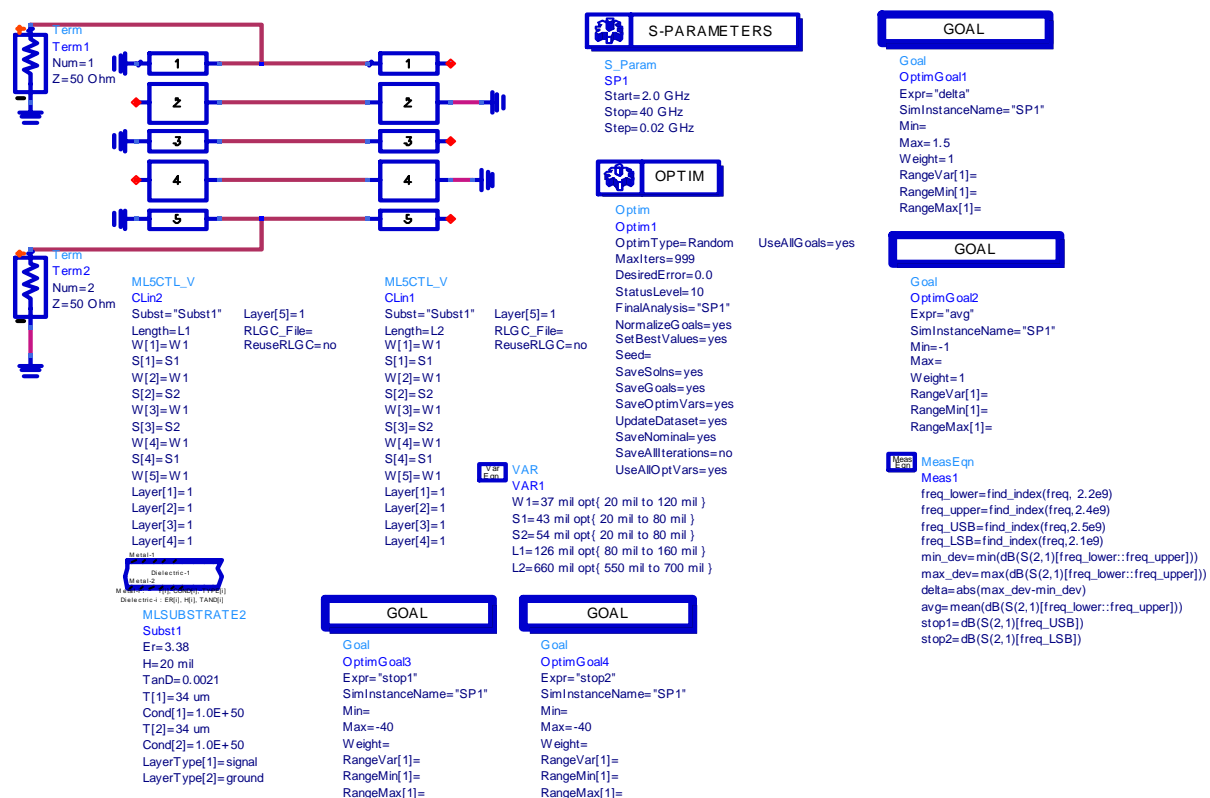


Figure 13: 5th-Order Optimization Circuit

The results obtained for the 5th-order filter after optimization are shown in Figure 14. For brevity, the 3rd-order optimization results are not shown (final simulation results for both filters will be included at the end of this section). As can be seen from Figure 14, the maximum dip in the passband is 1.5 dB—a dramatic improvement over that obtained with the wizard. Also, the rolloff of the filter is steeper.

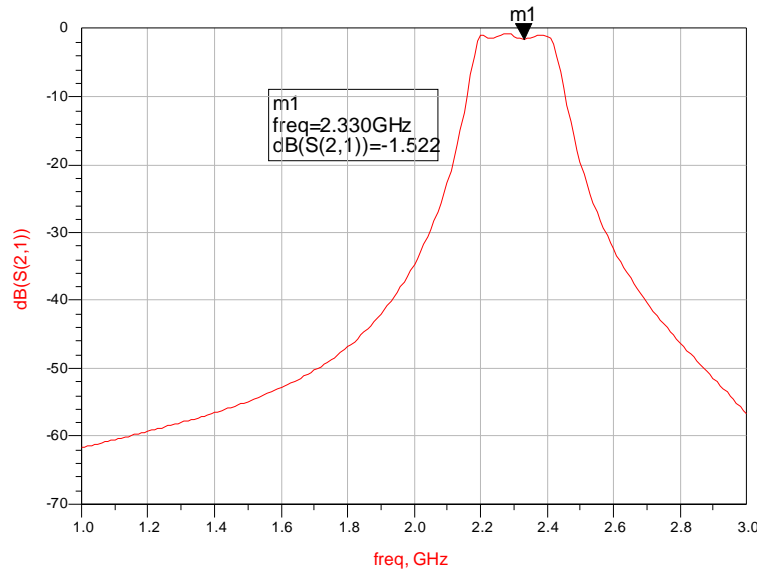


Figure 14: 5th-Order Filter Response using ADS Optimization

As a final verification of the filter design, a more accurate simulation was performed using Momentum. Momentum is a 2.5d RF electromagnetic simulator packaged with ADS. This allows for relatively quick simulation of the designed filters by importing the filter design into Momentum. Figure 15 shows an example layout of the 5th-order filter imported into Momentum. Some necessary changes were made to make the layout realizable; for example, the ground vias were made circular. As a result, the lengthwise dimensions had to be slightly lengthened to compensate. The final simulation results of both the 3rd-order and 5th-order filters are given by Figures 16 and 17, respectively. These results are acceptable, and this completes the discussion of the filter design.

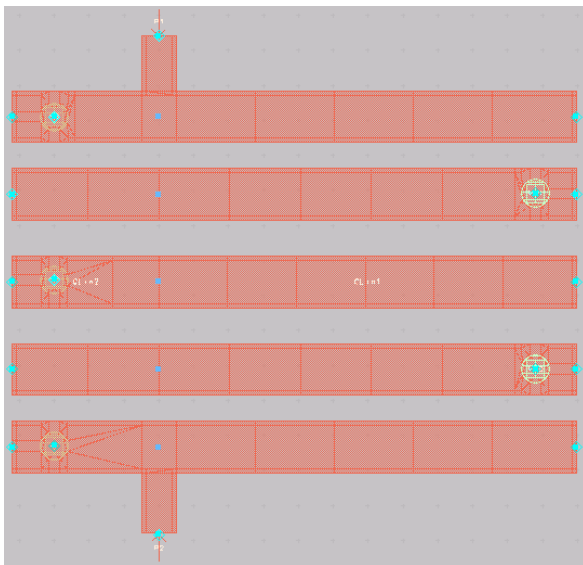


Figure 15: 5th-Order Filter Layout in Momentum

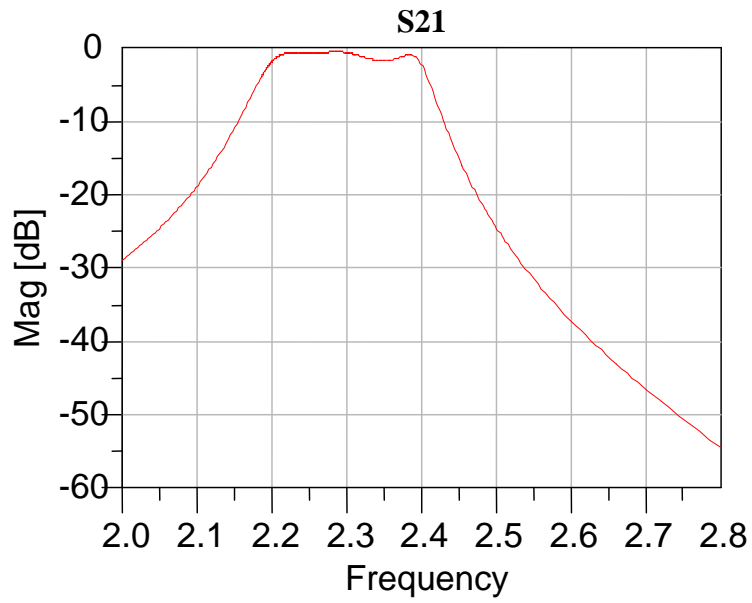


Figure 16: 3rd-Order Filter Frequency Response in Momentum

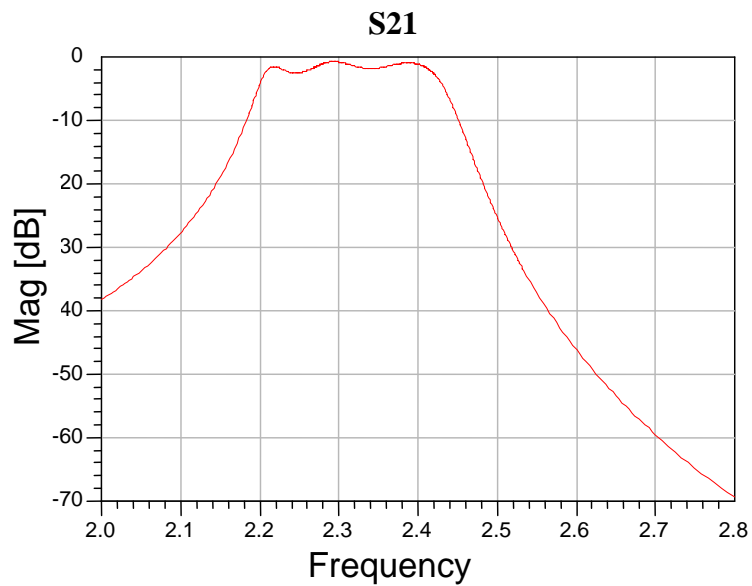


Figure 17: 5th-Order Filter Frequency Response in Momentum

Conceptual Redesign of Antenna Element PCB

Steering Redesign

The following design objectives will be addressed in this sub-section:

- Maximize steering angle
- Variable beamwidth (controllable)

The original configuration obtained steering through the use of two phase shifters. Each phase shifter only allows for a maximum phase shift ~110 degrees. This yields a total maximum phase shift of 220 degrees. To increase the steering angle, a larger phase shift is needed. Upon consultation with the manufacturer, SVMicrowave, by utilizing three phase shifters in series, a full 360 degrees of phase shift should be obtainable. The only sacrifice being made is an extra 1.3 dB of insertion loss.

Another way to maximize the steering angle is to more accurately control the phase shift. The original configuration used an analog voltage divider circuit in order to control each phase shifter's phase shift. This limited the maximum delta phase shift to ~30 degrees; as a result, the maximum steering angle is ~20 degrees. Also, the analog control assumes that the delta phase shift is linear with respect to voltage. Unfortunately, the linearity of the phase shifter's voltage response curve is mediocre at best (see [1] for details). In order to overcome these weaknesses, and add more flexibility in beam control, the phase shifters in the new design will be individually controlled by the digital control system. This will allow for digital linearity compensation and added flexibility via arbitrary phase control.

The second objective listed is to add variable beamwidth control. In order to vary the beamwidth, a tapered distribution of weights is required. (Each weight is multiplied by the incoming signal of each element, and then summed together.) The comparison made in most antenna textbooks is that a tapered distribution is mathematically analogous to windowing of a Fourier series. Therefore, a tapered distribution will have a wider beamwidth and lower sidelobes. The original configuration only changed the phase of each received signal, with no tapering. Tapering of the weights is to be obtained in the new configuration through the utilization of variable gain amplification on each antenna element. These will be controlled by the digital control system. Figure 18 shows the modified block diagram of the antenna element's PCB to include an additional phase shifter, digital control of each phase shifter, and variable gain amplification. Figure 19 shows a top system level diagram. Lastly, for reference, Figure 20 shows a block diagram of the RF signal processor.

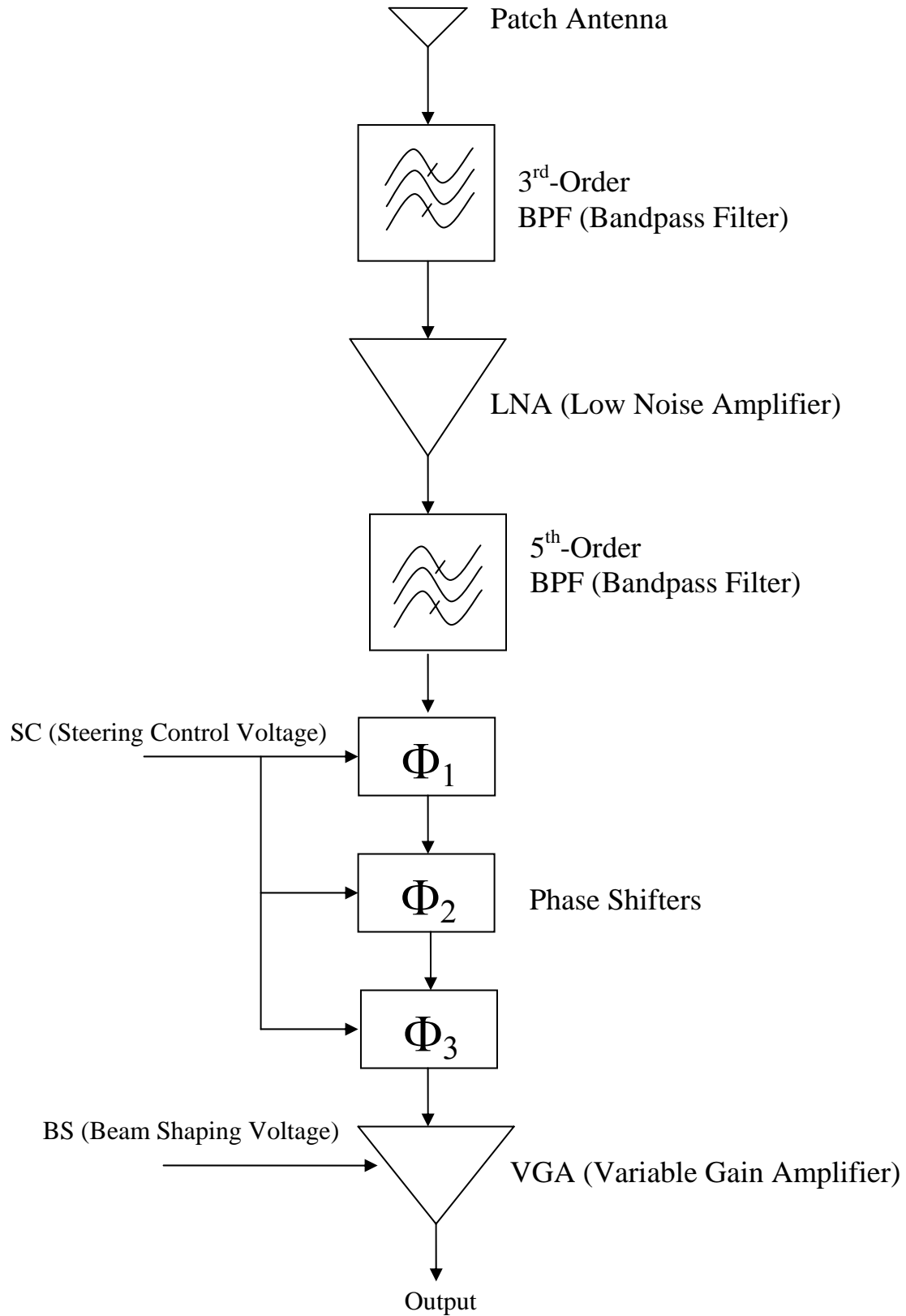


Figure 18: Block Diagram of a Modified Antenna Element

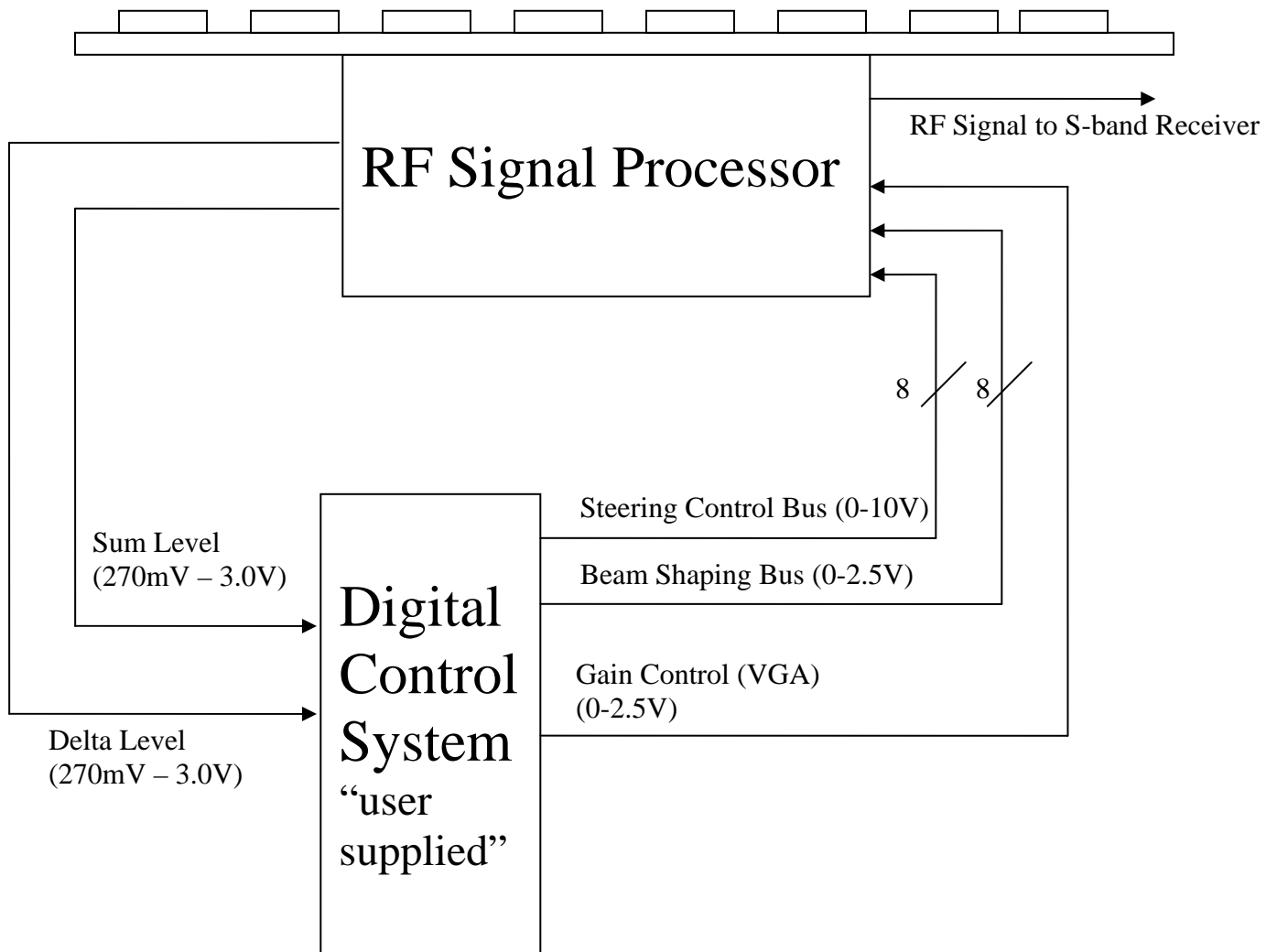
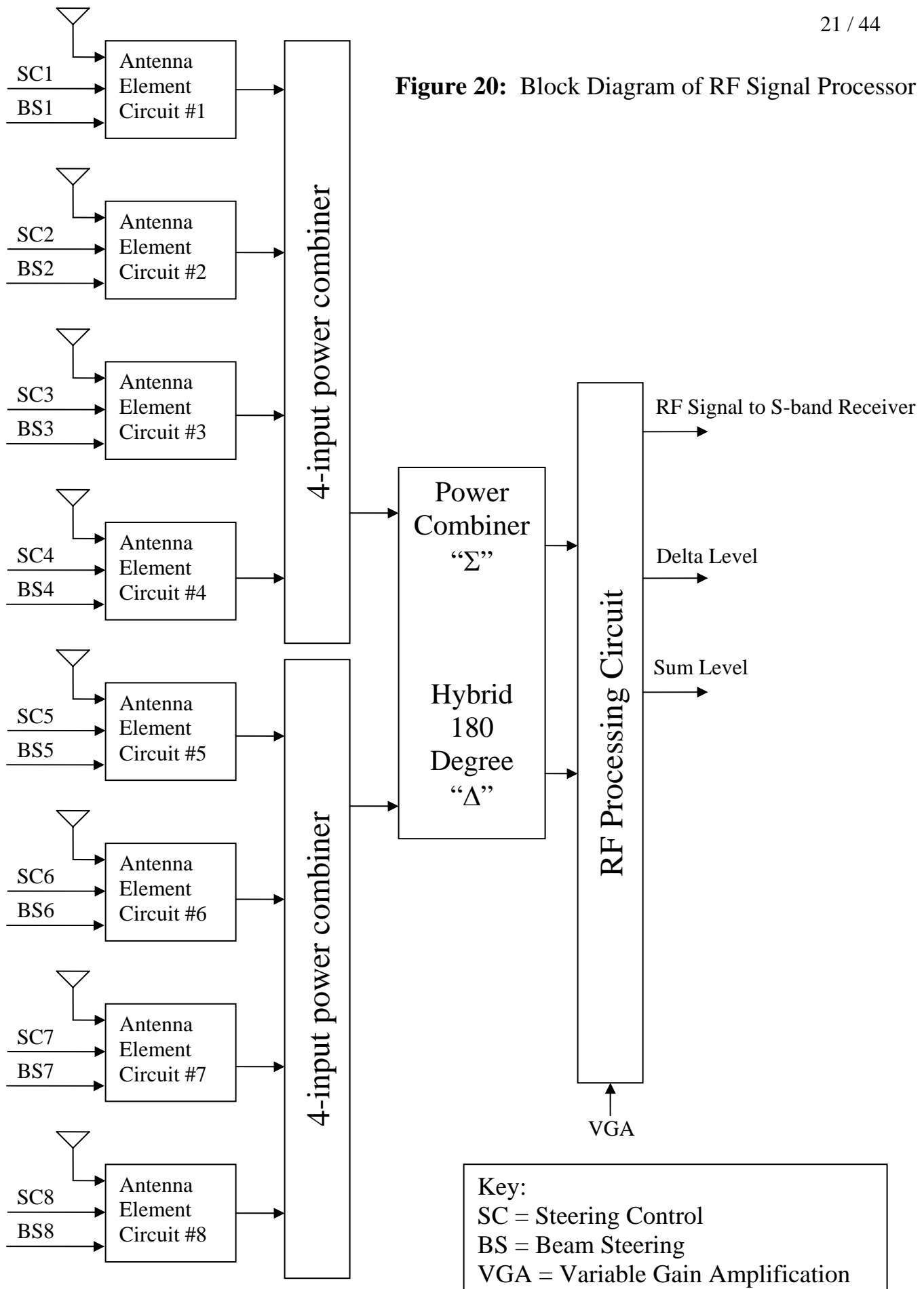


Figure 19: Block Diagram of a Modified System



We are now in a position to simulate the generated beam pattern obtained from both the antenna element and the weighted summer. It can be shown that both the element beam pattern and the array beam pattern may be multiplied together to form the composite beam pattern. In the simulations to follow, the array beam pattern has been normalized to yield 0 dB in the direction of arrival. One may envision a constant 9 dB added to the simulated plots in order to take into account the array gain associated with adding all elements together. This would describe the overall antenna gain with respect to an isotropic antenna. Nevertheless, the following plots accurately show the shape of the beam pattern. The first simulation will not use a tapered distribution. The beam pattern will be calculated at steering angles (relative to broadside) of 0, 30, 60, and 90 degrees. Figure 21 shows the results. As can be seen from Figure 21, when the beam is steered to 90 degrees, the element's beam patterns starts to attenuate the composite gain. Also, the peak radiation is not at the steering angle since the element's beam pattern is strongly distorting the composite beam pattern. For comparison, a maximum gain of 2.1 dB is achieved for a steering angle of 60 degrees. The actual realized steering angle is 48 degrees. On the other hand, a maximum of gain of ~6.25 dB is achieved for a steering angle of $\theta=0$ degrees (relative to broadside). Values for all angles are tabulated in Table 1.

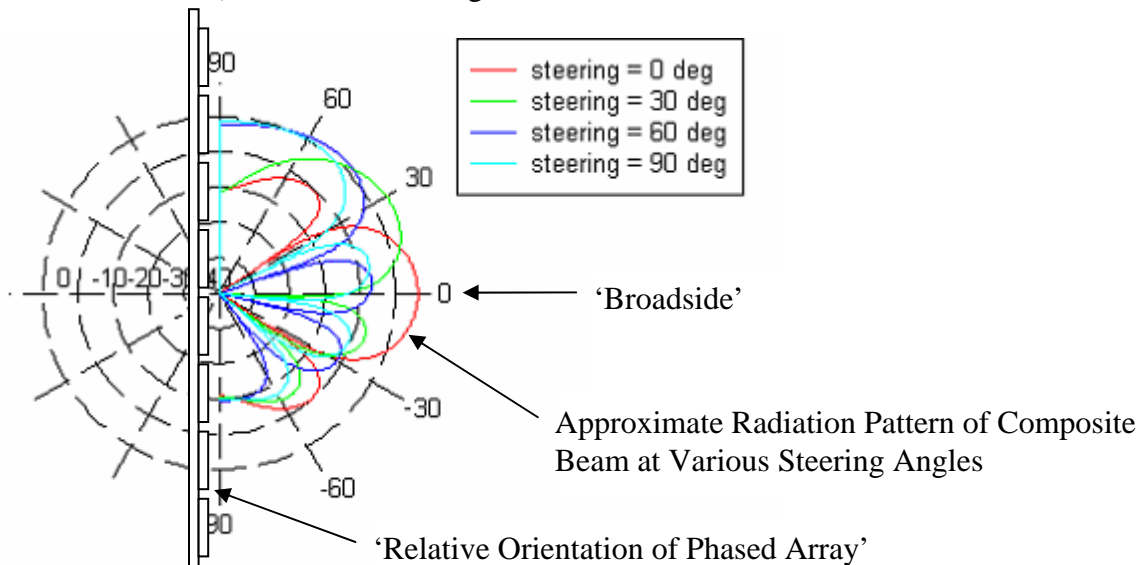


Figure 21: Simulated gain for various steering angles, using a uniform distribution

Steering Angle (deg)	3-dB Beamwidth (deg)	Maximum Gain (dB)	Realized Steering Angle (deg)	Sidelobe Level (dB)
0	27.5	6.3	0	-10.5
30	30.2	5.0	25.9	-7.0
60	42.1	2.1	47.9	-6.5
90	49.1	0.35	57.8	-6.7

Table 1: Tabulated parameters of simulated gain for various steering angles, using a uniform distribution

The second simulation will use a tapered distribution. The tapered distribution to be used is the Kaiser distribution, with Beta=3 [8, p 107]. A larger value of beta will increase the main beamwidth and decrease the sidelobe level. As in Figure 17, the beam pattern will be calculated at steering angles (relative to broadside) of 0, 30, 60, and 90 degrees. Figure 22 shows the results. As one would expect, the element's beam pattern still distorts the array's beam pattern. By comparison to Figure 21, the beamwidth has widened. Also, one observes substantially lower side lobes. It should be noted that the peak gain is lower. This is a consequence of the variable gain amplifiers being turned down to obtain a tapered distribution. Still, by close observation, the gain is greater than that obtained in Figure 21 over a broader range of angles. Table 2 contains tabulated values of various parameters for comparison with Table 1.

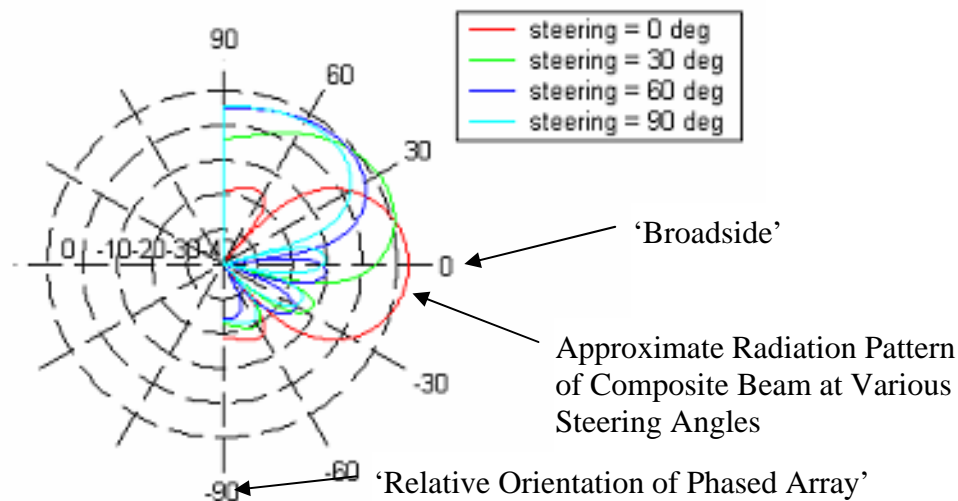


Figure 22: Simulated gain for various steering angles, using a Kaiser tapered distribution

Steering Angle (deg)	3-dB Beamwidth (deg)	Maximum Gain (dB)	Realized Steering Angle (deg)	Sidelobe Level (dB)
0	32.9	3.2	0	-26.8
30	35.6	2.0	24.5	-21.6
60	46.4	-0.76	44.5	-20.5
90	55.8	-2.3	52.9	-20.5

Table 2: Tabulated parameters of simulated gain for various steering angles, using a tapered distribution

Schematic Redesign

The following design objectives will be addressed in this sub-section:

- Increase dynamic range

In this subsection, the Antenna Element's schematic will be modified to incorporate the discussed changes. Minimal changes will be necessary for the new RF Signal Processor board, so no discussion of the RF Signal Processor board is given (notably, only the removal of the analog phase shifter voltage section will be necessary). The addition of a variable gain amplifier will improve the dynamic range of the system. The implementation of the schematic into ADS will be briefly discussed. Some components were simplified (with the proper use of engineering judgment) in order to allow implementation in a timely manner.

Figure 23 shows a top level view of the antenna element's schematic. The antenna is connected directly to port 1. Both the 3rd- and 5th-order filters are modeled using the previously discussed design. AMP1 and AMP2 use a manufacturer-supplied model. The VP242D phase shifters are modeled using their scattering parameters. There is approximately 1.3 dB of insertion loss for each. The phase shift may be manually controlled for each phase shifter. Unfortunately, it was not possible to easily convert the DC supplied phase shift control voltage into a phase shift due to limitations of ADS software. The only feasible method for doing this would have involved custom C-programming within the ADS environment. Lastly, the BGA2031 variable gain amplifier is modeled using a system level amplifier. The P1dB point and scattering parameters are incorporated from the datasheet. The amplifier specification sheet for BGA2031 described its small-scale nonlinear distortion using the term ACPR (Adjacent Channel Power Rejection). Unfortunately, this is not easily convertible to a TOI (Third Order Intercept) value for insertion into the system level amplifier. (The third order intercept is the theoretical output power of the desired signal when it would be equal to the third harmonic.)

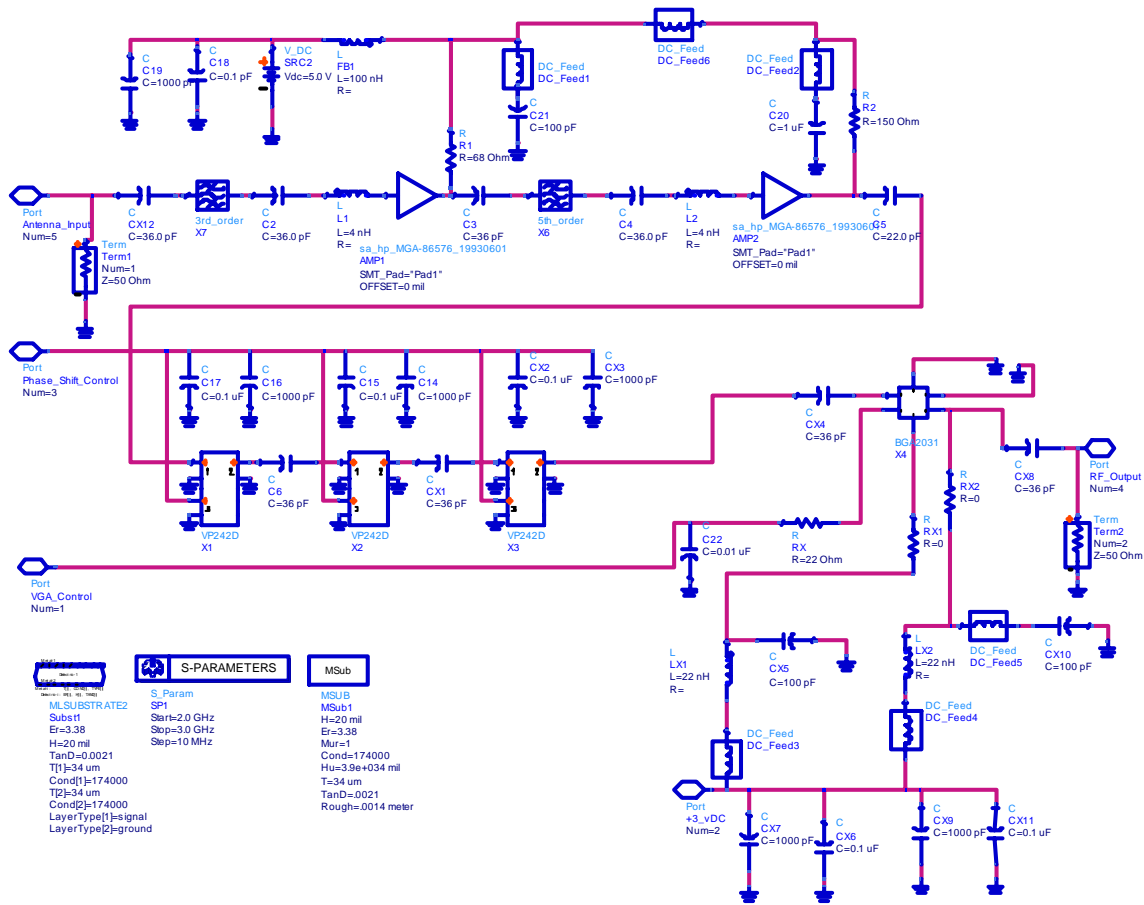
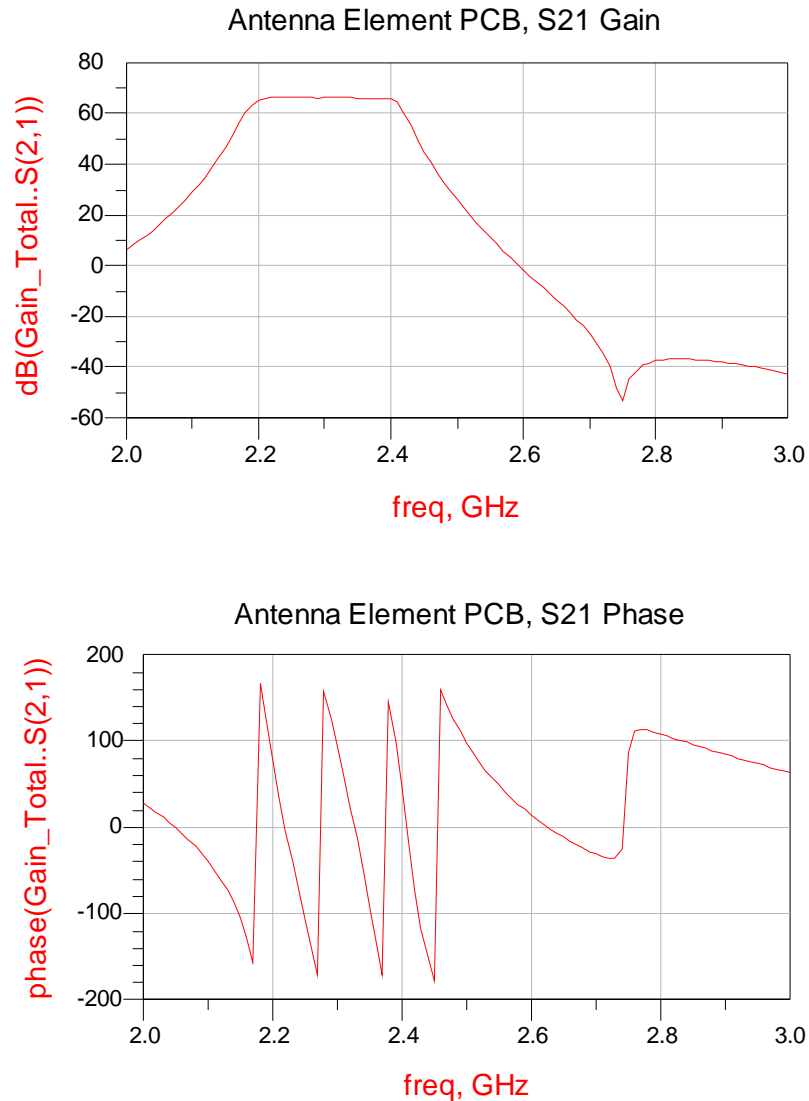


Figure 23: Top-Level Schematic of Antenna Element

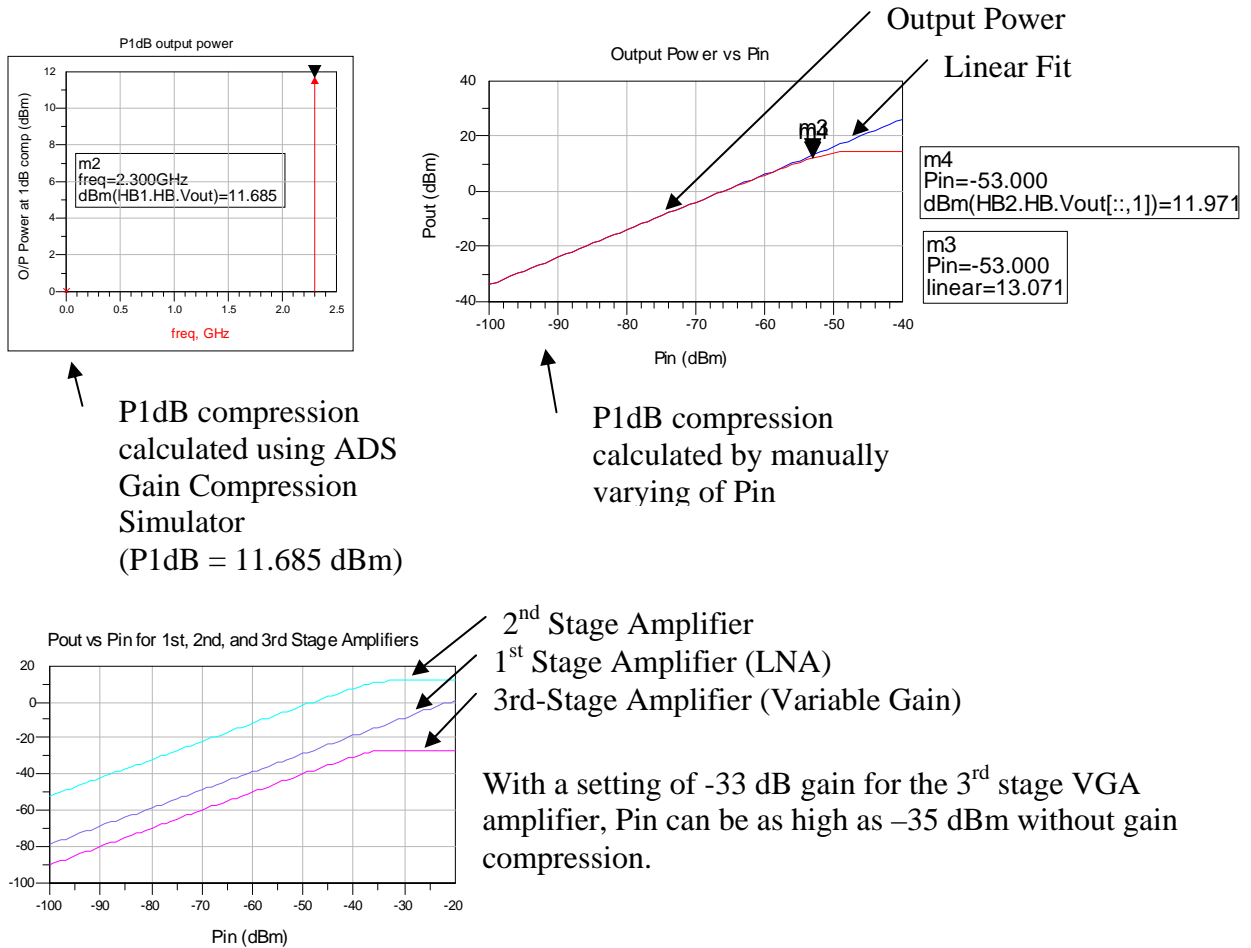
The following set of tests was executed. Results are described within the corresponding figures:

- Gain. The overall system gain was measured. Figure 24.
- Gain Compression. The power level for the system experiencing 1 dB of gain compression was computed. Figure 25.
- Noise Figure. The overall noise figure of the system with the various contributors. Figure 26.
- Intermodulation. The system receives two tones at maximum power of -35 dBm. The simulator calculates the resulting mixer terms within the system bandwidth. Figure 27.



The overall system gain is ~65 dB within the passband of the receiver. Approximately 65dB of attenuation occurs for a signal falling outside of the passband by 200 MHz. It should be noted that an additional 20 dB of variable gain is available in the RF signal processor.

Figure 24: Overall System Gain vs Frequency



P1dB compression calculated using ADS Gain Compression Simulator (P1dB = 11.685 dBm)

P1dB compression calculated by manually varying of Pin

With a setting of -33 dB gain for the 3rd stage VGA amplifier, Pin can be as high as -35 dBm without gain compression.

Figure 25: Gain Compression of System

The P1dB output power is 11.69 dBm. With the 3rd-stage VGA amplifier set to maximum setting, Pin can be as high as -53 dB without gain compression. With the 3rd-stage amplifier set to its minimum setting, Pin can be as high as -35 dBm without gain compression.

freq	nf		
	nf(1)	nf(2)	
2.200GHz	3000.000		2.494
2.225GHz	3000.000		2.445
2.250GHz	3000.000		2.705
2.275GHz	3000.000		2.412
2.300GHz	3000.000		2.121
2.325GHz	3000.000		2.408
2.350GHz	3000.000		2.853
2.375GHz	3000.000		2.672
2.400GHz	3000.000		2.867

Noise_Figure1..port1.NC.freq	Noise_Figure1..port1.NC.name	Noise_Figure1..port1.NC.type	Noise_Figure1..port1.NC.vnc
2.300GHz	AMP1.a1	Amplifier	200.1pV
	AMP2.a1	Amplifier	1.132pV
	R1	R	85.55fV
	X1.S2P2	S_Port	16.53fV
	X6.CLin1	PC_Line	917.5fV
	X6.CLin2	PC_Line	544.9fV
	X7.CLin1	PC_Line	129.0pV
	X7.CLin2	PC_Line	41.55pV
	_total	_total	241.7pV

Noise Figure Contributions 

Figure 26: Noise Figure of System

The system noise figure is 2.12 dB at 2.3 GHz. As to be expected the major contributor is the first stage LNA. The noise figure of the LNA is ~2 dB.

Mixing Products Included in Simulation

freq	Mix		
	Mix(1)	Mix(2)	
0.0000 Hz		0	0
50.00MHz		-1	1
100.0MHz		-2	2
150.0MHz		-3	3
200.0MHz		-4	4
250.0MHz		-5	5
300.0MHz		-6	6
350.0MHz		-7	7
400.0MHz		-8	8
450.0MHz		-9	9
500.0MHz		-10	10
1.950GHz		10	-9
2.000GHz		9	-8
2.050GHz		8	-7
2.100GHz		7	-6
2.150GHz		6	-5
2.200GHz		5	-4
2.250GHz		4	-3
2.300GHz		3	-2
2.350GHz		2	-1
2.400GHz		1	0
2.450GHz		0	1
2.500GHz		-1	2
2.550GHz		-2	3
2.600GHz		-3	4

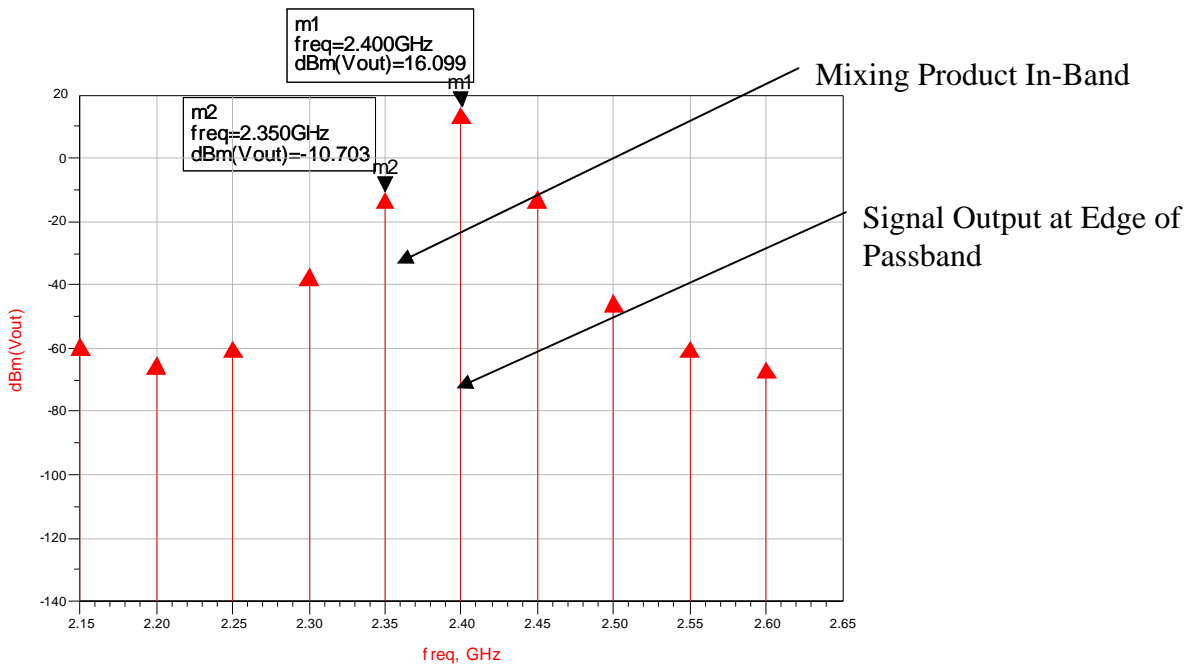


Figure 27: Intermodulation System Test

The input signals are 2.4 and 2.45 GHz tones at -35 dBm (the maximum signal level for the active antenna). As can be seen, there is ~26 dB of attenuation in the third order product.

Transmit Capabilities

The following design objectives will be addressed in this sub-section:

- Add dual mode capabilities – transmit & receive at 10 W
- Transmission and reception must operate in duplex mode

The ideal scenario would be to use the same antenna for both transmit and receive. Unfortunately, this is not possible. This is a result of the requirement that the antenna be able to send and receive simultaneously at the same frequency. The closest realization would have made use of an isolator. Due to the relatively poor mismatch of the antenna, reflected signal from the transmit circuit would overwhelm the receiver. No filtering could be used to attenuate the reflected signal since it is the same frequency as the receive section.

Upon consultation with the customer, it was decided to make the transmitter separate from the receiver. Consequently, the device would only be able to transmit. It was also decided that 8 W of transmit power was adequate. An additional requirement to transmit through a range of 1 mW thru 8 W was added.

Fortunately, the receive antenna would be able to reuse a large portion of the existing receiver design. Figures 28 and 29 show a block diagram of the preliminary design concept. Notice that the composite output ranges from 0.23 mW thru 8 W. The low side of 0.23 mW will allow tapering of the elements when operating at the minimal power of 1 mW. Unfortunately, the same is not true when operating at 8 W.

A brief description of the signal flow in Figures 28 and 29 follows. The modulated signal is amplified to a level such that the phase shifters in each antenna element will receive a signal level of ~ 0 dB of signal power after going through a splitter. This is a requirement of the phase shifters for optimal performance. The signal is then filtered to remove any spurious signals. Finally, the signal is amplified to 1 W (or the desired transmit power level) at each antenna element. As a result, the total radiated power is ~ 8 W (not including losses in the antenna structures). The customer is to provide a ‘driver amplifier’ that meets the listed specification: 50 dB dynamic range, -10 dB minimum gain, 40 dB maximum gain, 1 W maximum output. Further requirements of the ‘driver amplifier’ are listed in subsequent paragraphs.

To verify the calculations in Figures 28 and 29, a simplified schematic was incorporated into ADS. The implementation of the schematic into ADS will be briefly discussed. Some components were simplified in order to allow implementation in a timely manner. These will be briefly discussed. The power splitter was modeled by configuring multiple two-way splitters in series. An attenuator is placed within the power splitter circuit in order to simulate insertion loss. Although not explicitly used in the simulation, the power splitter’s model has an isolation of 20 dB. It is recommended that the cables connecting the splitter to the active elements be close to the same length ($\sim 3/100 \cdot \lambda$ or ~ 3 mm). This is not crucial since path length differences may be accounted for by proper adjustment of the phase

shifters. The power amplifier was modeled using a system amplifier. In addition to the previously discussed amplifier properties, the following were also incorporated. The amplifier has a NF (Noise Figure) of 5 dB, a 1 dB compression point of 30.2 dBm, and a 40 dBm TOI (Third Order Intercept). These specifications were obtained by comparison of a similar off the shelf component. In order to ensure adequate performance, these specifications should be met or exceeded. Lastly, both the 5th-order filter and VP242D phase shifters use the same model as that used in the receive antenna design.

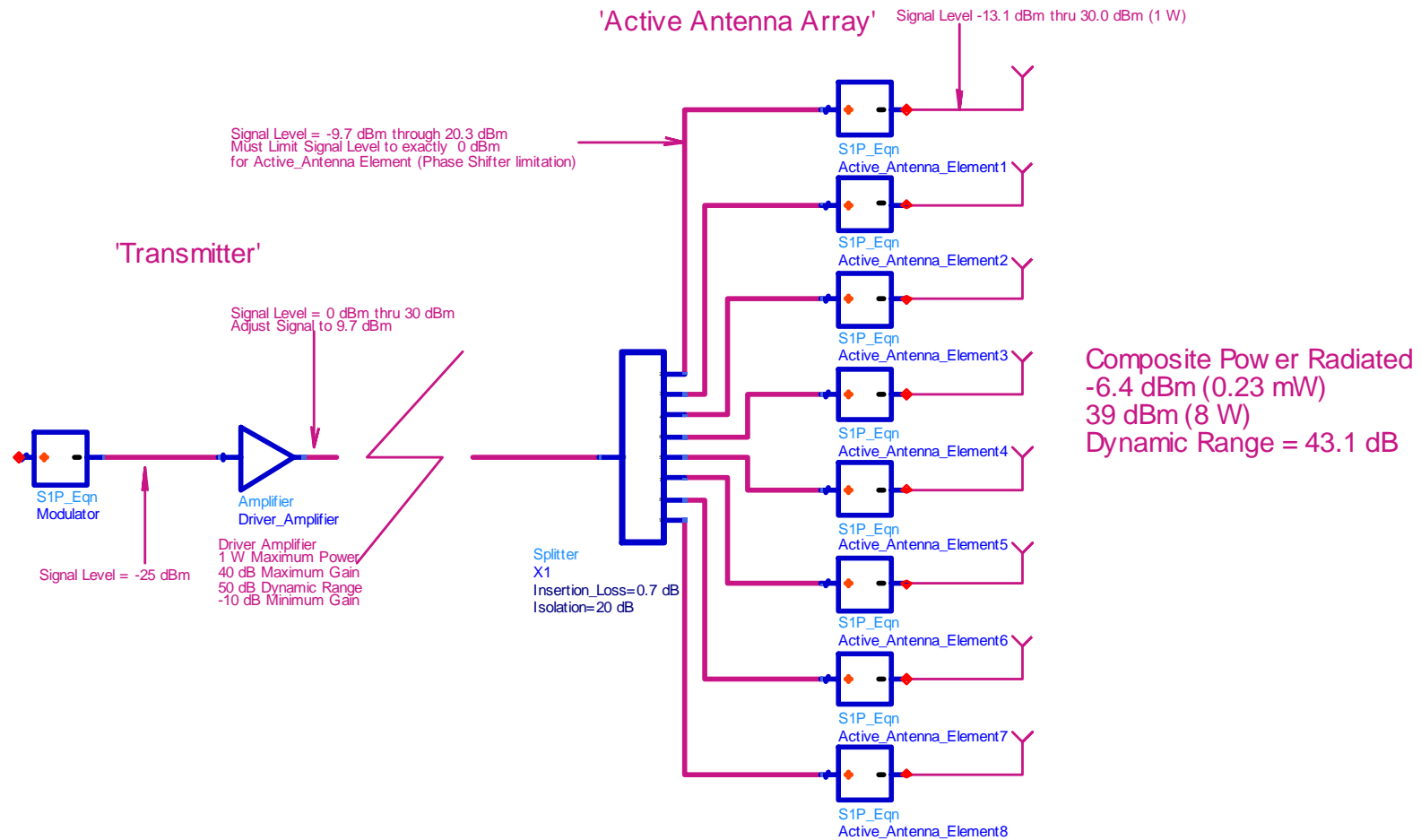


Figure 28: Top-Level Block Diagram of Active Antenna Array

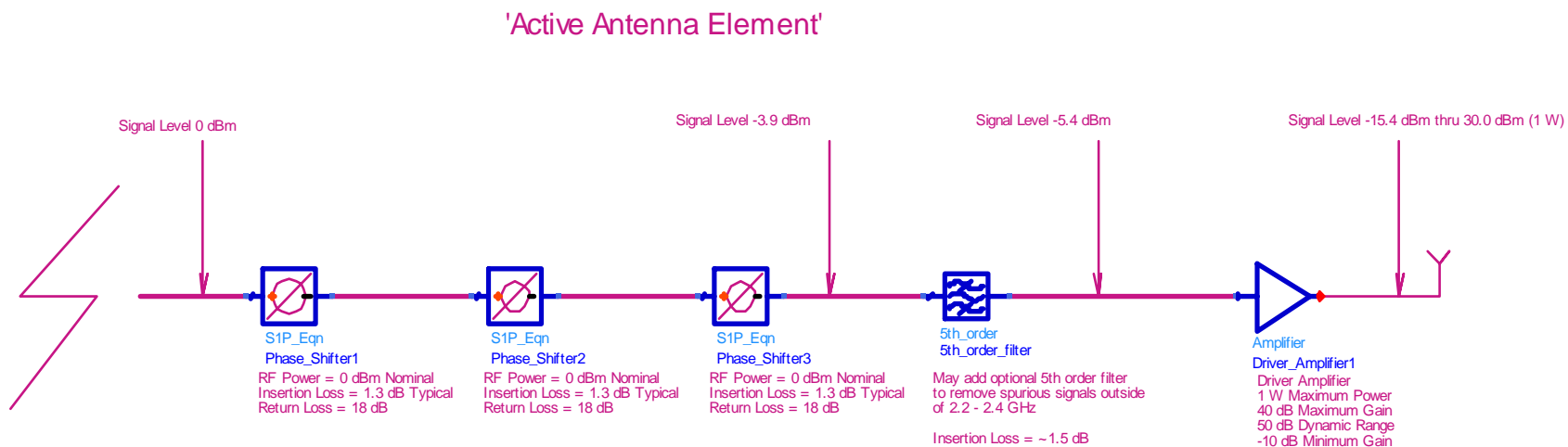


Figure 29: Top-Level Schematic of Active Antenna Element

The following set of tests was executed. Results are described within the corresponding figures:

- Gain. The overall system gain was measured. Figure 30.
- Gain Compression. The power level for the system experiencing 1 dB of gain compression was computed. Figure 31.
- Noise Figure. The overall noise figure of the system with the various contributors. Figure 32.
- Intermodulation. The system receives two tones from the modulator at maximum power, -28 dBm. The simulator calculates the resulting mixer terms within the system bandwidth. Figure 33.

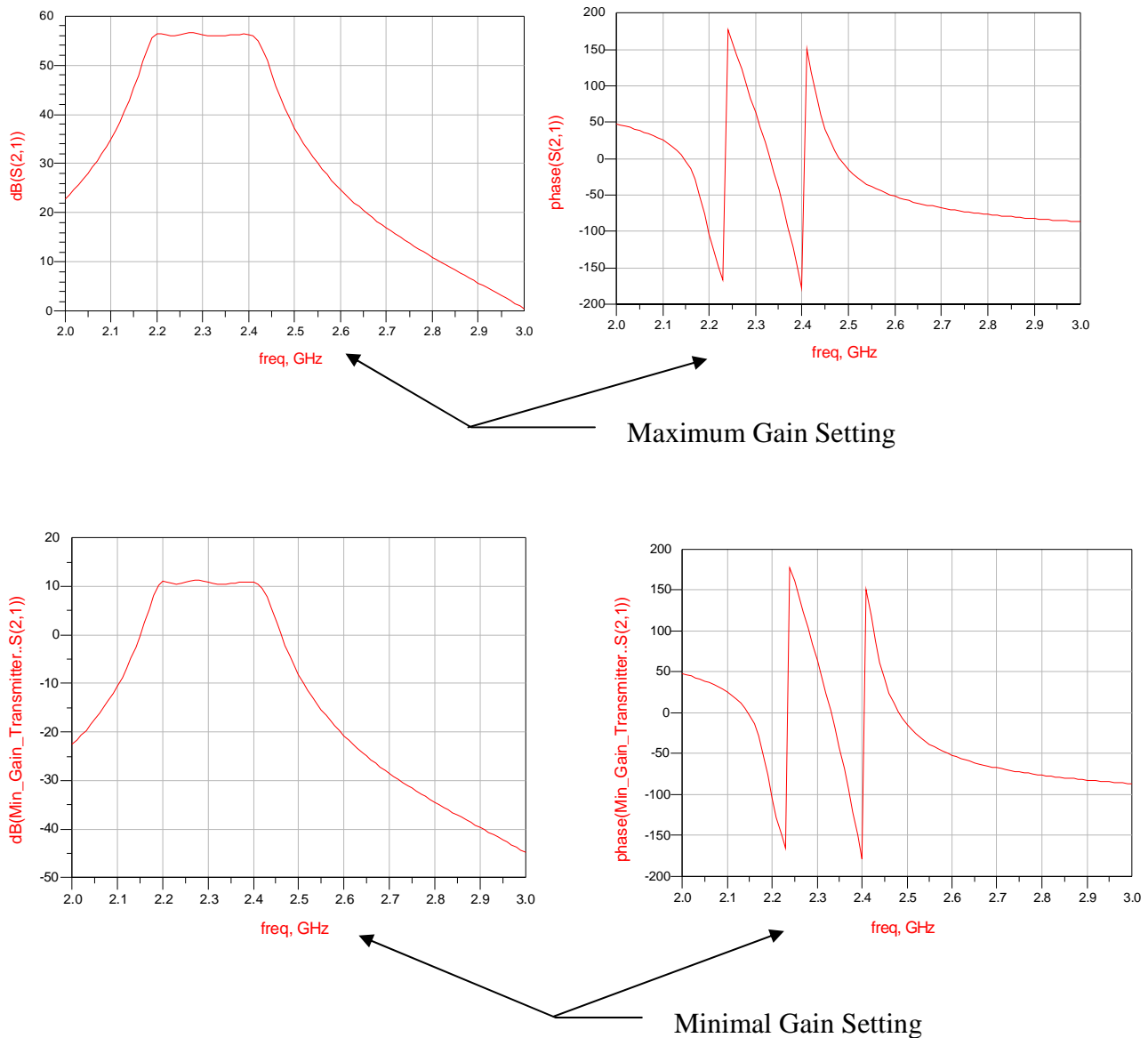


Figure 30: Overall Active Antenna Gain vs Frequency

With a maximum gain setting, the overall system gain is ~55 dB. With a modulated signal of -25 dBm, this will produce an output signal of 30 dBm, or 1 W. This is the output of one element. The composite power output will be 8 W. Similarly, for minimum gain setting, a modulated signal of -25 dBm will produce an output signal of -15 dBm, or 0.03 mW. This is the output of one element. The composite power output will be 0.24 mW.

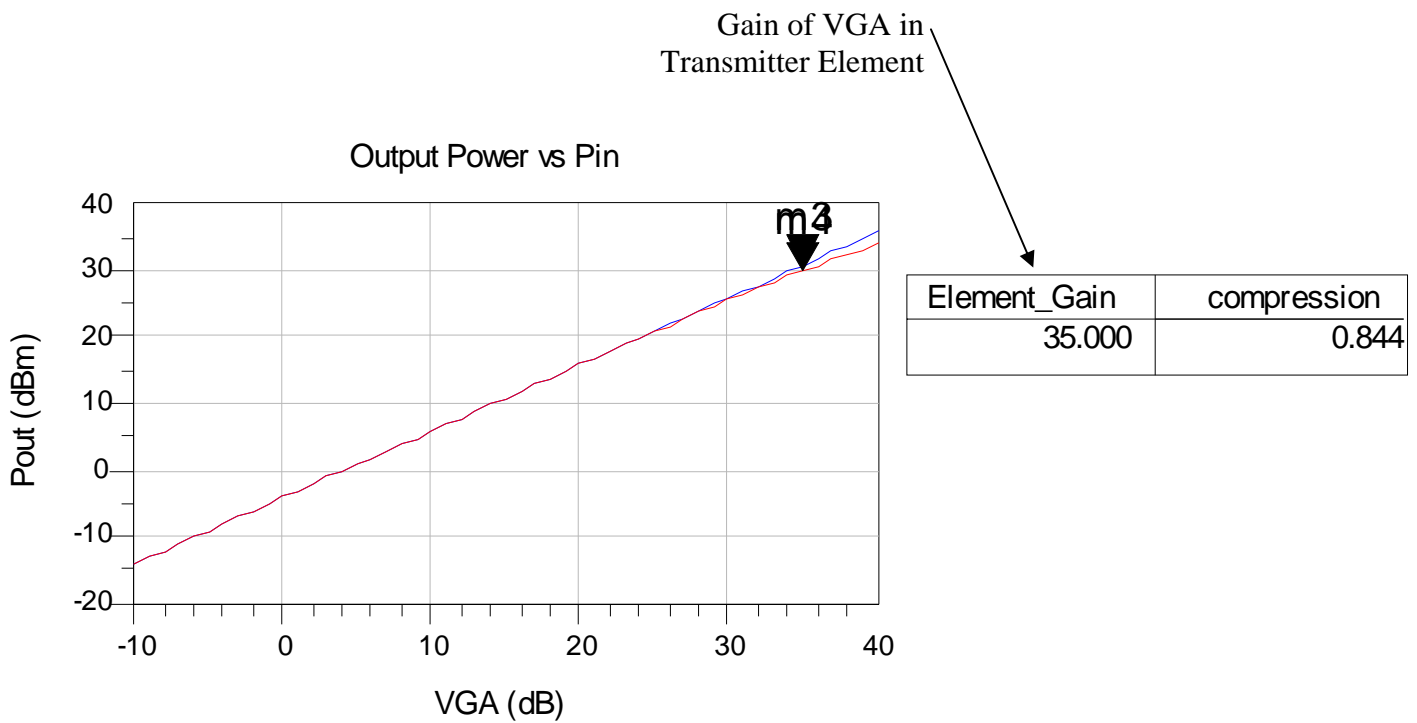


Figure 31: Gain Compression of Antenna Transmitter Element

The input power from the modulator is set to a constant of 25 dBm. The VGA (Variable Gain Amplifier) of the patch is varied. With the VGA set to 35 dB, the output power is ~30 dBm (1 W). Under this scenario, the transmitter is outputting maximum power. The amplifier is experiencing 0.844 dB of gain compression.

freq	nf		
	nf(1)		nf(2)
2.200GHz		0.000	5.034
2.225GHz		0.000	5.036
2.250GHz		0.000	5.035
2.275GHz		0.000	5.032
2.300GHz		0.000	5.035
2.325GHz		0.000	5.037
2.350GHz		0.000	5.036
2.375GHz		0.000	5.035
2.400GHz		0.000	5.036

...itter_Noise_Figure1..port2.NC.freq	...ter_Noise_Figure1..port2.NC.name	...itter_Noise_Figure1..port2.NC.type	...itter_Noise_Figure1..port2.NC.vnc
2.300GHz	total	total	428.6nV
	AMP1	Amplifier	426.1nV
	X2.AMP1	Amplifier	38.74nV
	X2.X3.S2P2	S_Port	12.06nV
	X1.PWR13.CMP1	S_Port	10.44nV
	X2.X2.S2P2	S_Port	10.39nV
	X2.X1.S2P2	S_Port	8.912nV
	X2.X4.CLin1	PC_Line	8.586nV
	X1.PWR11.CMP1	S_Port	7.110nV
	X2.X4.CLin2	PC_Line	4.819nV
	X1.PWR10.CMP1	S_Port	4.234nV
	X1.ATTEN1.CMP1	S_Port	2.262nV
	X3.X1.S2P2	S_Port	1.625nV
	X6.X1.S2P2	S_Port	1.625nV

Noise Figure Contributions

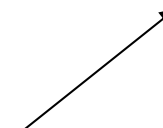


Figure 32: Noise Figure of Antenna Transmitter

The system noise figure is 5 dB. The primary contributor is the first stage driver amplifier before the power splitter. Since the system signal level is at 25 dBm, the noise figure should not introduce a significant amount of noise.

Mixing Products Included in Simulation

freq	Mix		
	Mix(1)	Mix	Mix(2)
0.0000 Hz		0	0
50.00MHz		-1	1
100.0MHz		-2	2
150.0MHz		-3	3
200.0MHz		-4	4
250.0MHz		-5	5
300.0MHz		-6	6
350.0MHz		-7	7
400.0MHz		-8	8
450.0MHz		-9	9
500.0MHz		-10	10
1.950GHz		10	-9
2.000GHz		9	-8
2.050GHz		8	-7
2.100GHz		7	-6
2.150GHz		6	-5
2.200GHz		5	-4
2.250GHz		4	-3
2.300GHz		3	-2
2.350GHz		2	-1
2.400GHz		1	0
2.450GHz		0	1
2.500GHz		-1	2
2.550GHz		-2	3
2.600GHz		-3	4

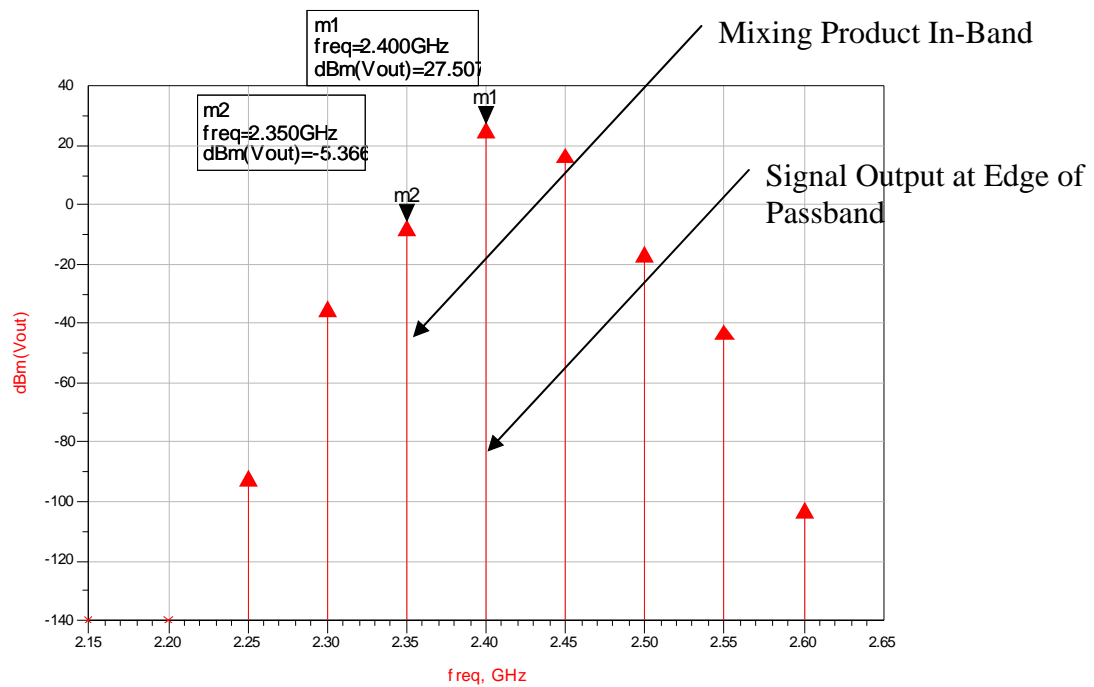


Figure 33: Intermodulation of Active Antenna

The input signals are 2.4 and 2.45 GHz tones at -28 dBm (the maximum signal level for the transmitter). As can be seen, there is ~33 dB of attenuation in the third order product.

Conclusions

For the presented conceptual redesign, it has been shown that all major redesign objectives have been met. The antenna bandwidth was increased to operate over the 2200-2400 MHz band. Simulations show that the new patch element meets this bandwidth yielding a VSWR less than or equal to 2 in the passband. This corresponds to approximately 90% of the power being transmitted at the edge of the passband. The bandpass filters were modified to accommodate the extended bandwidth. The antenna beamforming circuit has been modified to include digital control over both arbitrary phase and attenuation of each element. Simulations incorporating both the element and array beam pattern show that the beam may be steered to a realizable angle of 60 degrees from broadside. At a steering angle of 60 degrees, however, the main return axis is attenuated by ~6 dB. This is due to the limitations of the patch element's beam pattern. The receive antenna circuit was modified to accommodate an increased dynamic range. A simulation of the antenna revealed the capability of receiving a signal power as high as -35 dBm without overdriving the system. The gain of the receive system was shown to be ~65 dB with an additional 20 dB of variable gain within the RF signal processor. Other tests include a noise figure (2.1 dB) and an intermodulation test (~26 dB of suppression). Next, a block diagram design for an active transmit antenna was presented. Given that the discussed driver amplifier specification is met, the active antenna will be capable of transmitting within a range of 0.25 mW thru 8 W. As a second validation of the block diagram, a simulation in ADS was performed. The circuit demonstrated acceptable performance in a suite of tests to include gain, gain compression, noise figure and intermodulation. In conclusion, these results show that both a new receive antenna and an active transmit antenna should be capable of meeting the proposed redesign objectives.

Further Work

The following outline briefly summarizes anticipated future work with the second design iteration of the antenna array.

1. Build prototype of antenna element
 - a. Verify / Order required components
 - b. Calibration strategy
 - c. Complete board layout
 - i. Antenna element
 - ii. Signal processing board
 - iii. Patch antenna
 - d. Fabricate antenna
 - e. Calibrate and test antenna
 - f. Interconnect user supplied digital controller
 - g. Create desired adaptive beamforming algorithm

2. Build prototype of active antenna element (transmitter)
 - a. Complete design of driver amplifier
 - b. Verify / order required components
 - c. Calibration strategy
 - d. Complete board layout
 - i. Antenna element
 - ii. Signal processing board
 - iii. Fabricate antenna
 - e. Calibrate and test antenna
 - f. Interconnect user supplied digital controller
 - g. Create desired adaptive beamforming algorithm

3. Future enhancements
 - a. Possible to use same antenna for transmit and receive
 - i. Use different operating frequencies
 - ii. Isolate by using time division multiple access
 - b. Increase number of elements / size of antenna
 - i. May not be feasible given design constraints

References

- [1] Depardo, Dan, “2.3-2.4 GHz Phased-Array Prototype”, 2004.
- [2] Ulaby, Fawwaz; Moore, Richard; Fung, Adrian, *Microwave Remote Sensing Active and Passive*, Volume I, Norwood, MA: Artech House, 1981, p 160.
- [3] Huie, C. Keith, *Microstrip Antennas: Broadband Radiation Patterns Using Photonic Crystal Substrates*, 2002.
- [4] Stutzman, Warren L. & Gary A. Thiele. *Antenna Theory & Design*. New York, NY: John Wiley & Sons, Inc., 1998.
- [5] Balanis, C.A. *Antenna Theory: Analysis and Design*, John Wiley and Sons, New York, 1997.
- [6] *Ansoft High Frequency Structure Simulator v9 User's Guide*, Rev 2.0, Ansoft Corporation, Pittsburgh, PA, March 2004.
- [7] Matthaei, Young and Jones, *Microwave Filters, Impedance-Matching Networks, and Coupling Structures*, Artech House, 1980, pp. 614.
- [8] Van Trees, Harry L. *Optimum Array Processing, Part IV of Detection, Estimation, and Modulation Theory*. New York: John Wiley & Sons, Inc., 2002.
- [9] P. W. Hannan and M. A. Balfour, “Simulation of a phased-array antenna in waveguide,” *IEEE Trans. Antennas Propagat.*, vol. AP-13, pp. 342-345, May 1965.

Appendices

Appendix I: Matlab Code

Figure 9

```
%Written by: Russell Hofer
%March 2005
%Program Description: Approximate Element Beam Pattern

theta=-pi/2:.01:pi/2;

point1_db=6.32 %maximum value of realized gain (db)
point2_db=1.17 %realized gain at theta=60 degrees

maximum=10^(point1_db/20)
point2=10^(point2_db/20)
alpha=acos(point2/maximum)*2/(3^.5)

element=maximum*cos(alpha*sin(theta));
element_db=20*log10(element)

zero=20*log10(element)>0
element_db=element_db.*zero
polar(theta,element_db)
```

Figure 17, 18

```
%Written by: Russell Hofer
%March 2005
%Program Description: Consummate beam pattern at various steering
% angles Uniform or Tapered Weighting

N = 8; % Elements in array
d_cm = 2.9 % Element spacing in centimeters
d_m = d_cm/100; % Element spacing in meters
c = 3e8; % Speed of light
f = 2.3e9; % Nominal frequency of array
lambda = c/f;
d = d_m/lambda; % spacing wrt wavelength
steering = 90 % steering angle in degrees (90 =
broadside)
Beta = 0 % Beta = 0 => not tapered,
positive value => tapered

D=d*[-(N-1)/2:1:(N-1)/2]; % element locations
ang = pi*[-1:0.001:1];
u = cos(ang);

%calculate an approximate beam pattern for an element
```

```

theta=pi*[-1/2:.001:(1/2-.001)]; %temporary variable used to calculate
element beam pattern
point1_db=6.32 %maximum value of realized gain (db)
point2_db=1.17 %realized gain at theta=60 degrees

maximum=10^(point1_db/20)
point2=10^(point2_db/20);
alpha=acos(point2/maximum)*2/(3^.5);

element=maximum*cos(alpha*sin(theta));
element=[0:.001:1]*0,element]; %necessary to align coordinate system
of element

count=0
for steering=[0,30,60,90] %steering relative to broadside

steering=90-steering %transform steering, 90 degrees = broadside
count=count+1

AS = exp(j*2*pi*cos(steering/180*pi)*D') %Steering, phase portion
AB = ones(N,1)/N %Beamforming, amplitude
portion

if Beta~=0 %Use bessel distribution if
tapered
for i=0:(N-1)
n_tilda=i-(N-1)/2;
expression=Beta*sqrt(1-(2*n_tilda/N)^2)
AB(i+1)=besseli(0,expression)
end
end

W = AS.*AB %Weight vector including steering
W=W/max(abs(AB))/N %Normalize weights so max is 1/N

Au = exp(j*2*pi*D'*u);
B = W'*Au

B = B.*element %Incorporate element beam pattern to form
consummate beam pattern

G = 20*log10((abs(B)));
figure(1)

if count==1
h=polardb(ang,G,-50,'r');
elseif count==2
h=polardb(ang,G,-50,'g');
elseif count==3
h=polardb(ang,G,-50,'b');
elseif count==4
h=polardb(ang,G,-50,'c');
end
hold on
end

```

```
legend('',' ',' ',' ',' ',' ',' ',' ',' ',' ',' ',' ','steering = 0 deg','steering =  
30 deg','steering = 60 deg','steering = 90 deg')
```